Dating groundwater in the surrounding of Sakatti exploration target area in order to understand groundwater recharge and water interactions

Kuutti Koskimaa
5/2020
Master's thesis
Department of geosciences and geography
Master program in geology and geophysics
University of Helsinki

HELSINGIN YLIOPISTO
HELSINGFORS UNIVERSITET
UNIVERSITY OF HELSINKI

Tiedekunta/Osasto Fakultet/Sektion – Faculty Faculty of science	Osasto/Institution– Department Department of geosciences and geography / Master's Programme in Geology and Geophysics	
Tekijä/Författare – Author Juho Kuutti Ilmari Koskimaa		
Työn nimi / Arbetets titel – Title Dating groundwater in the surrounding of Sakatti exploration target area in order to understand groundwater recharge and water interactions		
Oppiaine /Läroämne – Subject Hydrogeology and Environmental Geology		
Työn laji/Arbetets art – Level Master's thesis	Aika/Datum – Month and year 5/2020	Sivumäärä/ Sidoantal – Number of pages 60

Tiivistelmä/Referat – Abstract

AA Sakatti Mining Oy is researching the possibility of conducting mining operations in Sakatti ore deposit, located partially under the protected Viiankiaapa mire. In order to understand the waters in mining development site, the interactions of surface waters, shallow aquifers, and deep bedrock groundwaters must be understood. To estimate these interactions, hydrogeochemical characterization, together with four tracer methods were used: Tritium/helium, dichlorodifluoromethane and sulfur hexafluoride, stable isotopes of hydrogen and oxygen, and carbon-14.

Most of the shallow groundwater samples are similar to the natural precipitation and groundwater in their chemical composition, being of Calcium bicarbonate type. B-11-17HYD013 was an exception, containing much more Cl and SO_4. The samples from the deep 17MOS8193 all show a very typical composition for this type of a borehole, on the line between the saline Sodium sulphate and Sodium chloride water types. The samples from the 12MOS8102, as well as the river water samples and the Rytikuru spring sample are located between these two end members.

The hydrogen and oxygen isotope values divided the samples into two distinct groups: those that show evaporation signal in the source water, and those that do not. The most likely source for the evaporated signal in the groundwaters is in the surface water pools in the Viiankiaapa mire, which have then infiltrated into the groundwater and followed the known groundwater flow gradient into the observation wells near the River Kitinen.

Tritium showed no inclusion of recently recharged water in the deep 17MOS8193, and dated most of the shallow wells with screen below bedrock surface to be recharged in the 70's and 80's. B-10-17HYD017 had an older apparent age from 1955, and B-14-17HYD006 was curiously dated to be recharged in 2018.

^{14}C gave apparent age of over 30 000 a for the deep 17MOS8193. The slight contents of ^{14}C could be caused by slight contamination during sampling meaning the age is a minimum. The sample M-4-12MOS8102 got an apparent age of ~3 500 a, which could in turn be an overestimate due to ancient carbon being dissolved from the local bedrock fractures.

CFC-12 showed apparent recharge dates from 1963 to 1975 in the shallow wells, and no recently recharged water in the deep 17MOS8193, and so was generally in line with the ^{14}C and Tritium results, although some contamination had happened. SF_6 concentrations exceeded possible concentrations considering other results, most likely due to underground generation, and the method was dismissed.

By trace element composition, all samples from the deep 17MOS8139 are distinct from other samples and saw slight dilution in concentrations of most elements in the span of the test pumping. Other samples are more mixed and difficult to interpret, but some trends and connections are visible, such as the higher contents in wells with screens below the bedrock surface than those with screens above the bedrock surface, and the exceptionally high contents of many elements in B-13-17HYD004.

Overall, the study did benefit from the large array of methods, showing no interaction between the deep bedrock groundwaters and shallow groundwaters or surface waters. The evaporated signal from the Viiankiaapa was clearly visible in the samples close to the River Kitinen.

Avainsanat – Nyckelord – Keywords
Hydrogeology, Hydrogeochemistry, hydrochemistry, groundwater dating, Sakatti, tritium, carbon-14, CFC-12, SF6, Isotope

Säilytyspaikka – Förvaringställe – Where deposited
HELDA

Muita tietoja – Övriga uppgifter – Additional information

TABLE OF CONTENTS

1. INTRODUCTION

After discovering the significance of the Sakatti Ni-Cu-PGE deposit just north of Sodankylä in Northern Finland (Brownscombe *et al.* 2015), mining company AA Sakatti Mining Oy has extensively researched the possibility of conducting mining operations without straining the local protected and fragile mire environment. Therefore, the interaction between surface water, shallow aquifer groundwater as well as water in deep bedrock environment in the vicinity of the deposit and planned operation area must be understood.

To study these interactions and recharge age of water in different hydrostratigraphic units, several groundwater dating methods were used together with hydrogeochemical characterization including various field and laboratory measurements, such as ion chemistry and trace element analysis. The data was examined both statistically and graphically.

According to Healy (2010), groundwater recharge is defined as a downward flow of water adding to the groundwater in the saturated zone underneath, either from precipitation or a surficial body of water, such as a river or a lake. Groundwater age means the time passed since the water came isolated from the atmosphere. Recharge age estimation is an important and potent tool in determining the connections and interactions between different storages of groundwater, identifying different sources of recharge and providing information of flow paths.

Groundwater recharge age can be estimated using various tracer components (Fig. 1). Four different tracer methods were chosen based on their availability, dating range to cover as long time periods as is relevant in this study, and ability to cross check each other: anthropogenic tritium and helium ($^{3}H/^{3}He$) and dichlorodifluoromethane and sulfur hexafluoride (CFC-12/SF_6), and naturally occurring stable isotopes of hydrogen and oxygen ($\delta^{2}H$, $\delta^{18}O$) and carbon-14 (^{14}C). ^{14}C method was selected for its ability to recognize ancient groundwaters thousands of years old (Kalin 2000), which were expected to be found from the deepest boreholes. The anthropogenic tracers, ^{3}H, CFC

and SF_6 are not found in groundwaters recharged before the 1940–50s, save for some exceptions, so their mere existence in a sample indicates a component of water recharged within the last 70 years (Plummer and Busenberg 2006). The stable isotopes of hydrogen and oxygen show whether the water has been subject to evaporation before infiltration, thus hinting at its origins before permeation (Gat and Tzur 1967, Gonfiantini 1986).

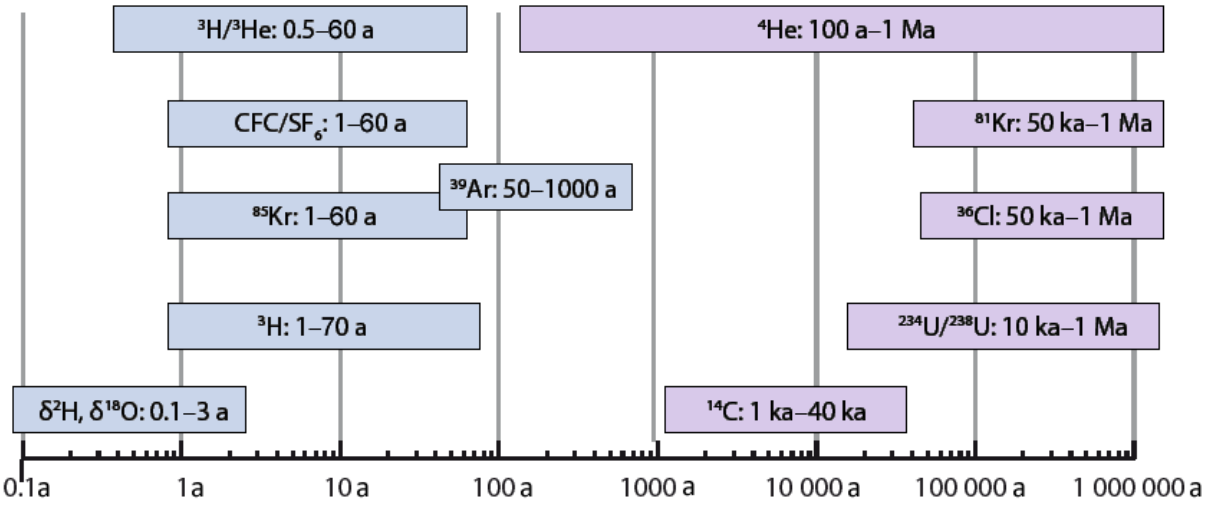

Figure 1. Isotope and chemical tracers in use for estimating groundwater age (based on International Atomic Energy Agency 2013. Ages modified to better suit present time).

In the simplest model of a groundwater system, a piston flow, water would enter the system, and keep going onwards or stay in the reservoir without mixing (Bethke and Johnson 2008). All water at a certain point would be of one age. However, groundwater is almost always mixed from various components of differing origin and age (Healy 2010). While looking at the results of this study, it must be kept in mind that the apparent age of groundwater represents the proportional average subsurface residence time of the components of the water, which in most cases isn't the exact time of the recharge. The concentrations of different tracer elements used with each method can also vary due to various processes, such as adsorption, dissolution or degradation (Plummer 2005). Therefore, multiple dating methods are required to obtain meaningful hydrogeological data and determine the groundwater forming components.

A great part of this study is to determine, whether the deep (~1 000 m) bedrock groundwaters in the area interact with shallow groundwaters or surface waters. Similar deep groundwaters have been studied in Finland before. According to Blomqvist (1999), Finnish groundwaters in the upper part of the bedrock are typically recently recharged bicarbonate waters similarly to precipitation, with low (<1 000 mg l^{-1}) total dissolved solids (TDS), while going deeper they are usually thousands or tens of thousands of years old, of sulphate or chloride type with much higher TDS (1-170 g l^{-1}) and often around 5 000 mg l^{-1} of dissolved chloride. The $\delta^{18}O$ values vary on a wide scale from -7 ‰ to -17 ‰, and $H^2\delta$ values from -40 ‰ to -130 ‰ locating close to the Global Meteoric Water Line (GMWL, Craig 1961). According to Blomqvist *et al.* (1987), the $\delta^{18}O$ and $H^2\delta$ values sometimes diminish with increasing depth, but exceptions are common and depend on the geochemical properties and evolution at different depths. The change from fresh to saline water usually happens around 300-600 m (Blomqvist 1999). For example, according to Ahonen *et al.* (2011), electrical conductivity and salinity of Outokumpu Deep Drill Hole R2500 raised rapidly in the first 225 m, then increased slowly until depth of 1 000 m, after which it decreased. TDS was about 12 000 mg l^{-1} in depths of 200-1 000 m, increasing to ~50 000 mg l^{-1} at the bottom of the borehole at a depth of 2516 m. Ca, Na and Cl were the main dissolved components.

This study adds understanding of groundwater recharge and mixing of various waters from different hydrostratigraphic units using groundwater dating methods combined with hydrogeochemical characterization. It aims to answer the question of groundwater age in shallow sedimentary aquifers, in the fractured upper bedrock as well as in ~1 000 m deep bedrock basal thrust, and also the potential interaction between these units and surficial waters.

2. STUDY SITE

The study area is located in Sodankylä municipality, 16 km north of Sodankylä town. In 2009, mining company Anglo American discovered a substantial magmatic Ni-Cu-PGE-Au deposit beneath the Viiankiaapa mire, and later in 2012 two smaller satellite deposits, one north-east and the other south-west of the main deposit (Fig. 2) (Brownscombe *et al.* 2015). Due to the mire being under Natura 2000 and mire conservation act protections (Metsähallitus 2006), the detailed environmental studies and precautions as well as comprehensive understanding of the local surface water and groundwater flow patterns are required.

2.1 Bedrock

The study area is in the Paleoproterozoic Central Lapland Greenstone Belt, which consists of volcanic and sedimentary rocks formed on top of archaic granite and gneiss. According to Brownscombe *et al.* 2015, the host rock of the main deposit, as well as the two smaller deposits, is olivine ortho-meso-adcumulate rock, overlain by carbonate breccia and fine-grained mafic units. The hanging wall consists of komatiitic basalts, and the footwall of mica schists, quartzites and carbonate rocks. The upper parts of the bedrock are partially fractured, faulted and occasionally chemically weathered (Hirvas 1991 and Åberg *et al.* 2019a), which potentially enables and affects groundwater flow patterns. A groundwater flow model (Modelmuse graphical user interface software (USGS) and MODFLOW-NWT (Niswonger *et al.* 2011)) by Åberg *et al.* (2019) indicates in a potential groundwater connection from the Viiankiaapa mire to the river through possible bedrock fractures of the bedrock, although the extent is still unknown due to the uncertainties in the hydraulic properties of the fractures. The major faults and fractures, and schistosity of the bedrock are almost vertical.

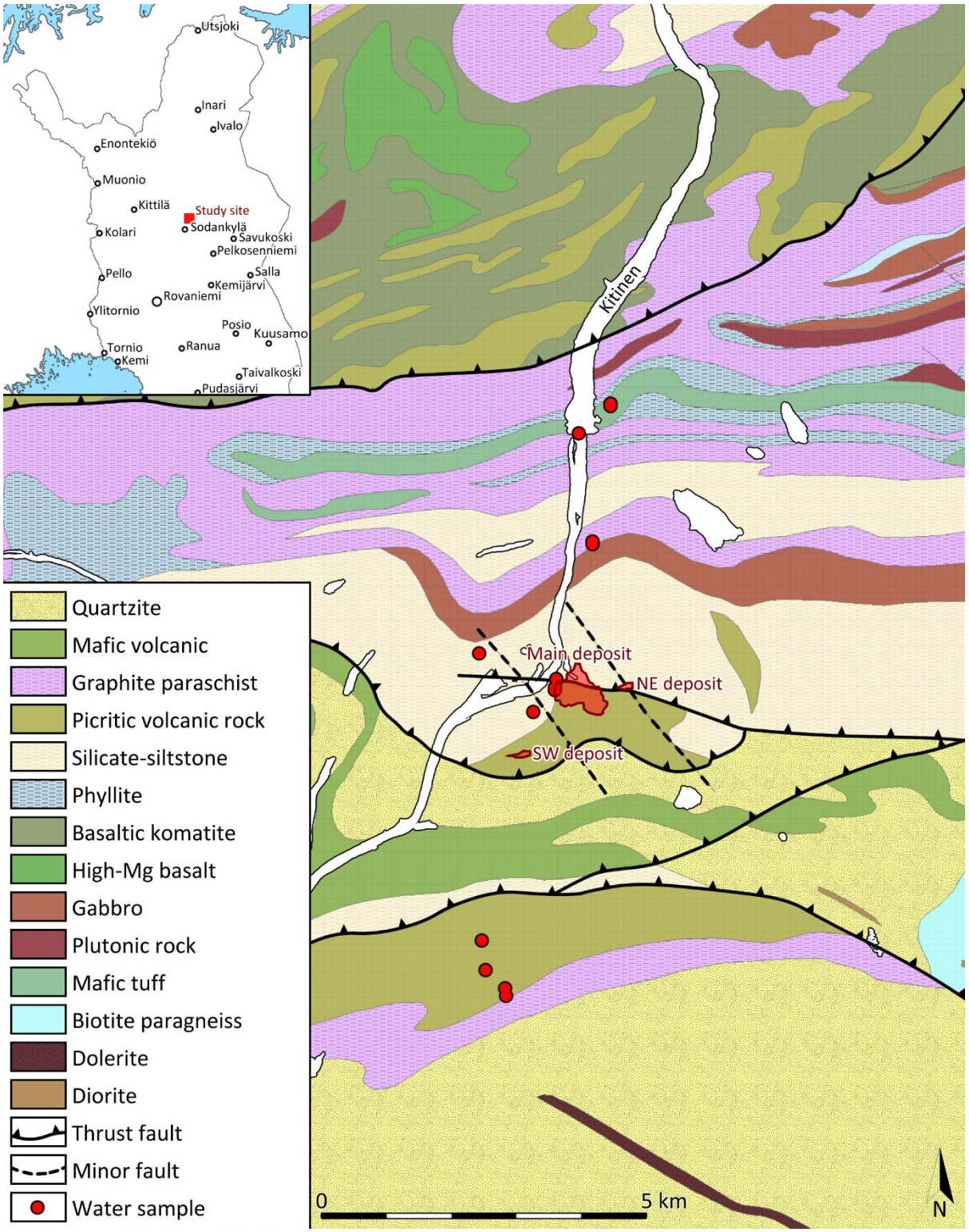

Figure 2. Location of the study site and a bedrock map of the study area (based on Geological Survey of Finland 2017).

2.2 Surficial deposits

The topography of the study area is mostly rather flat, varying between 180–200 m above sea level, with a few hills being 50–90 m higher. The surficial deposits vary in thickness from 0 to 41 m, median being 9.1 m (Åberg A. *et al.* 2017). The Quaternary surficial deposits in the vicinity of the River Kitinen are mostly gravel, sand and moraine. The flat floodplains consist of a peat layer with average thickness of 2.3 m (Åberg A. *et al.* 2017).

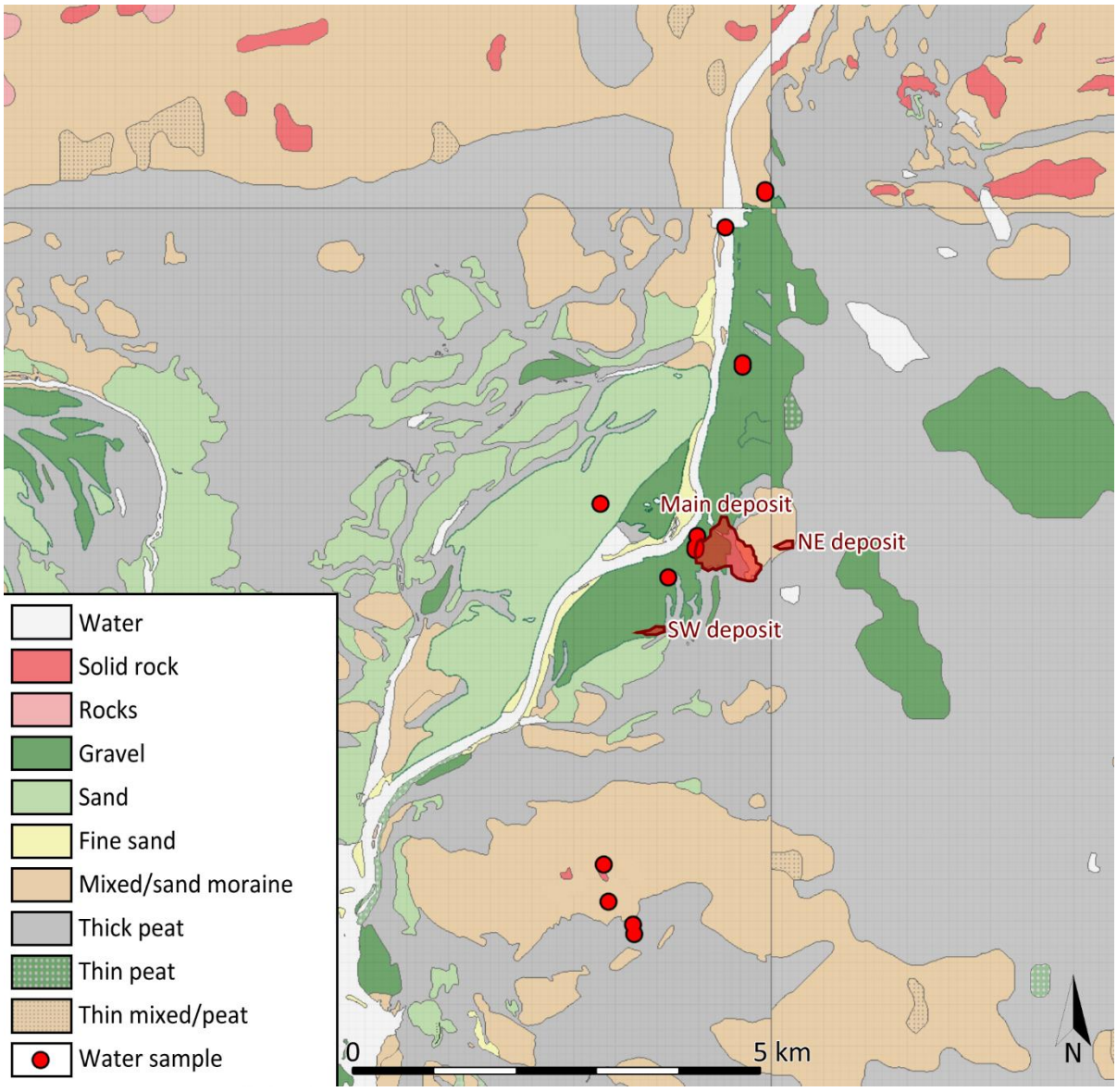

Figure 3. A soil map of the study area (based on Geological Survey of Finland 2010).

2.3 Surface waters and groundwaters

Based on studies by Åberg S. *et al.* (2017) and Åberg *et al.* (2019) the aquifers are small and scattered. In some locations, the low hydraulic conductivity of till units causes forming of small perched aquifers. The River Kitinen runs through the study area from north to south-west, originating from the lake Porttipahta 50 km upriver. Seven power plants have been constructed along the River Kitinen since the 1960s, Kelukoski power plant in 2001 being the last one. Especially the water flow regulation of Porttipahta and Lokka reservoirs has significantly reduced the previously extensive spring floods of the mires (Alanne *et al.* 2014) and surface water infiltration to groundwater. Surface water and groundwater flow patterns in the area have been significantly affected by this change (Åberg S *et al.* 2017, Åberg *et al.* 2019b).

In the current state, Åberg S. *et al.* (2017) modelled both the surface water and groundwater flows to be towards the River Kitinen in the western part of the Viiankiaapa mire. Åberg *et al.* (2019) modelled groundwater discharge in the banks of the River Kitinen, as well as within the mire area. Recharge was modelled to occur in the sorted sediments of the riverbanks, and occasionally on topographical elevations in the mire area.

3. MATERIALS AND METHODS

3.1 Samples

Water samples were collected from 19 different locations (Fig. 4, Table 1), with multiple samples from some locations e.g. from different depths or on different dates. Samples 1-8 were collected in 20.-22. of April 2018, and samples 10-21 were collected in 22.-24. of May 2018. A total of 27 sample sets were collected:

- 6 sample sets (orange, D) from the ~1 km deep 17MOS8193, collected on 14.4., 21.4., 27.4. and 29.4. in 2018 during the three weeks of pumping. The water was flowing to the borehole from a basal thrust in a depth of ~850–940 m.

- 4 sample sets (black, M) representing different depths (M-1 23, M-4 65 and M-2 96 m) of the borehole well 12MOS8102, adjacent to the borehole 17MOS8193.
- 7 sample sets (yellow, B) from 10–250 m deep groundwater wells, with screens below the bedrock level.
- 6 sample sets (green, G) from 5–15 m deep groundwater wells with screens above the bedrock level (in sediment).
- 2 sample sets (dark blue, S) from the River Kitinen, S-7 taken from above the Matarakoski dam in April and S-21 taken from above the Kelukoski dam in May (to the south-west of the area, not visible on the map).
- 1 sample set (light blue, P) from Rytikuru, a spring that is likely to dry out during summer.
- 1 sample set (red, R) from groundwater discharging from a bank of the Ruosteoja ditch that leads the outflow from the pumping of borehole 17MOS8193 to the River Kitinen. These two results are not reviewed further, because they were only taken to check if the pumped water could still be identified in the analyses. The results are included in Appx. 2.

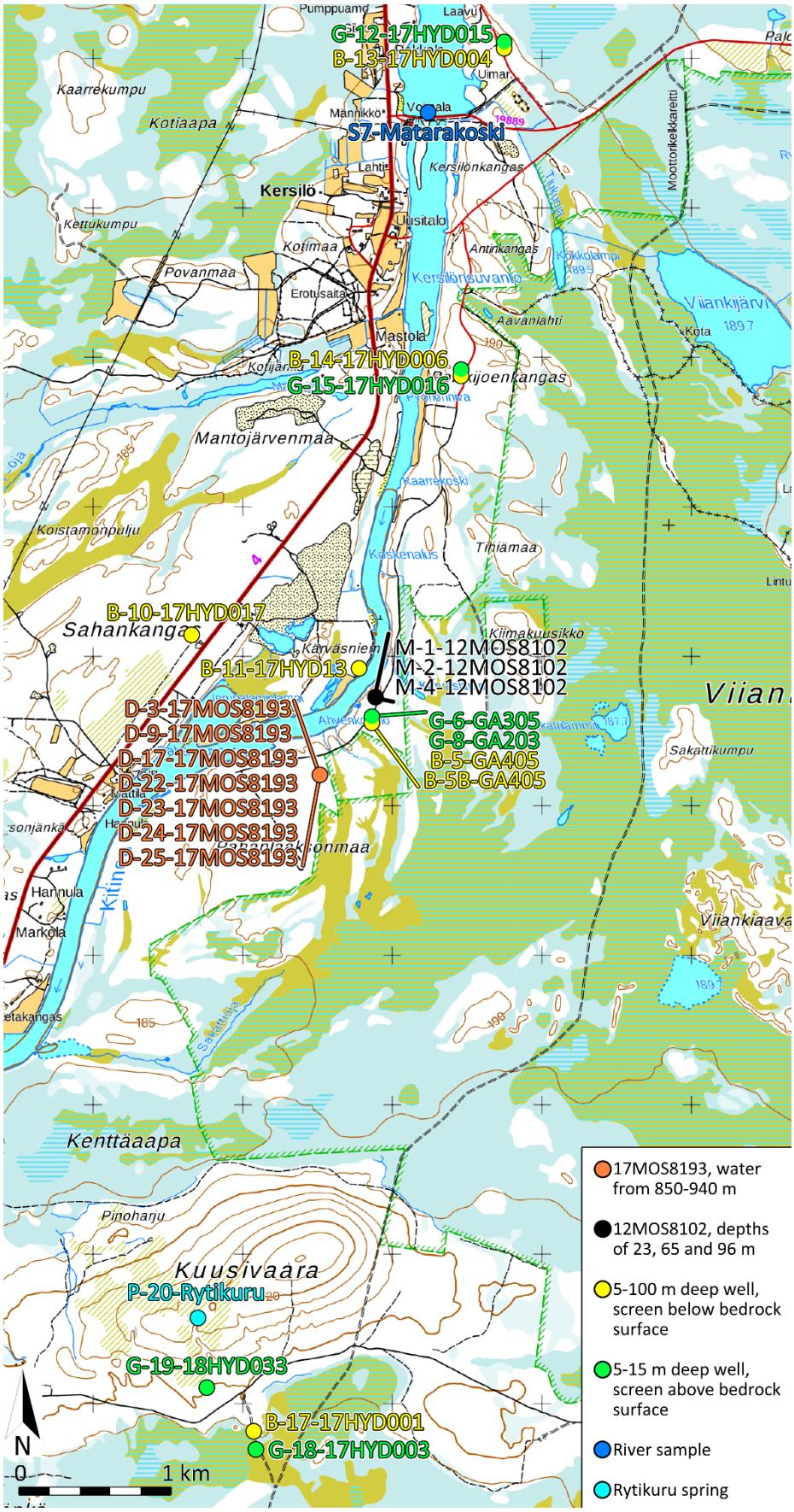

Figure 4. A map of the study area and the sample locations.

Water sampling was preformed from a deep (1000 m) basal thrust during test pumping performed by SRK, using a Grundfos BMI-MP1-230V pump from 100-300 m deep bedrock wells/boreholes, using pumps/bailers and Limnos sampler from shallow wells as well as surface waters, respectively. The depths, screen dimensions, bedrock levels, water levels and pump depths of most of the 5–250 m deep wells are presented in Appx. 1.

Figure 5. Grundfos BMI-MP1-230V pump flushing a well for the sample set B-10-17HYD017. May 2018.

Table 1. Collected samples and performed analyses.

	^{14}C	T/He	CFC-12 and SF_6	$\delta^2H/\delta^{18}O$	Ion chemistry	Trace elements
D-22-17MOS8193-1404					x	x
D-3-17MOS8193	x	x	x	x	x	x
D-23-17MOS8193-2104					x	x
D-24-17MOS8193-2704					x	x
D-9-17MOS8193-29A	x	x	x	x	x	x
D-25-17MOS8193-29B					x	x
M-1-12MOS8102 23 m				x		
M-1-12MOS8102 23 m		x	x		x	x
M-2-12MOS8102 96 m		x	x	x	x	x
M-4-12MOS8102 65 m	x	x	x	x	x	x
B-5-GA405 12 m		x				x
B-5B-GA405 12 m		x	x	x	x	x
B-10-17HYD017		x	x	x	x	x
B-11-17HYD013		x	x	x	x	x
B-13-17HYD004		x		x	x	x
B-14-17HYD006		x		x	x	x
B-17-17HYD001		x		x	x	x
G-6-GA305 9 m		x	x	x	x	x
G-8-GA203 4 m				x	x	x
G-12-17HYD015				x	x	x
G-15-17HYD016				x	x	x
G-18-17HYD003				x	x	x
G-19-18HYD033				x	x	x
P-20-Rytikuru				x	x	x
S-7-Matarakoski				x	x	x
S-21-Kelukoski				x	x	x

Before collecting any of the samples, the groundwater wells were flushed amply, so that the water in the well had changed multiple times. ^{14}C, T/He, CFC-12 and SF_6 samples were collected where they were deemed to be most useful, and some wells did not generate enough water for all samples in the sampling program (Table 1). Especially noble gas, CFC and SF_6 sampling requires a large volume of water in a short span of time. All samples were sealed using laboratory film prior to shipping/storing.

3.2 Groundwater dating methods

In the 20th century humans have released various substances to the atmosphere and hydrosphere, which have then spread around the world. These substances dissolve in

precipitation and are found in groundwaters formed from then on (Healy 2010). The most commonly used substances in recently recharged groundwater dating and tracing are anthropogenic tritium and chlorofluorocarbons (Solomon and Cook 2000, Plummer and Busenberg 2000), whereas carbon-14 is the most used tracer for dating samples recharged before human influence (Kalin 2000).

3.2.1 T/He

Tritium (^{3}H, T) occurs in groundwater as a part of water molecules ($^{1}H^{3}HO$). Concentrations of tritium are expressed as Tritium Units (TU), where 1 TU = 1 ^{3}H-atom/10^{18} atoms H. 1 TU = 0.118 Bq kg^{-1} (Healy 2010). Tritium is naturally generated by cosmic radiation, and as a product of natural decay of uranium and thorium (Bethke and Johnson 2008). Nuclear detonations since 1950s greatly increased the tritium concentrations in global precipitation, although the concentrations have since reached nearly natural levels (Schlosser *et al.* 1988). The tritium content in precipitation depends on the tritium content of the atmosphere. After the water is recharged into an aquifer, its tritium content starts to decrease as it beta-decays into ^{3}He with a half-life of 12.3 years (Bethke and Johnson 2008).

The age of a groundwater sample can be calculated from its contents of tritium and tritiogenic ^{3}He. Tritiogenic ^{3}He must be separated from ^{3}He in water in equilibrium with air, ^{3}He in excess air and radiogenic ^{3}He formed as a result of the decay of radioactive minerals (Schlosser *et al.* 1988). As the ratio of Ne and He contained in excess air can be assumed be equal to their atmospheric ratio, the concentration of neon is used to assist in determining the amount of ^{4}He in excess air (Schlosser *et al.* 1989). The amount of tritiogenic ^{3}He can then be estimated using the known average atmospheric $^{3}He/^{4}He$-ratio. The contents of radiogenic ^{3}He are calculated from the concentrations of radiogenic ^{4}He assuming a $^{3}He/^{4}He$ ratio of $2*10^{-8}$ (Schlosser *et al.* 1989, Plummer *et al.* 1993). The sum of the contents of remaining ^{3}H and the tritiogenic ^{3}He gives an estimate of the initial concentration of ^{3}H at the time of recharge. Comparison of the initial ^{3}H contents to the average tritium concentrations in the atmosphere at that time, gives a way to evaluate the correctness of the analysis.

Challenges

The contents of tritium in precipitation depends on not only its concentrations in the atmosphere, but also on latitude, the time of the year and the distance from coastal areas (Plummer *et al.* 1993). In certain conditions, some tritium may be generated underground as a decay product of radioactive minerals, and sometimes very high contents of helium generated in the bedrock can make the dating impossible (Solomon and Cook 2000, Heilweil *et al.* 2009).

Sampling

The tritium, helium and neon sample collection was performed according to instructions provided by Jürgen Sültenfuß (University of Bremen 2016), which are described below. Tritium samples were collected in 1 000 ml plastic containers. The bottles were flushed with low water pressure, with as little foaming and bubbling as possible. The bottles were amply spilled with sample water, before pouring out some water to leave some room for volume change and sealing the bottles. The bottles were then sealed with laboratory film.

For helium and neon analysis, two 40 ml Cu-tubes (Fig. 6) supported with an aluminium rack were filled for each sample. Each tube was connected to the pump with a transparent hose, with the diameter of the hoses decreasing in the flow direction. A short transparent hose was attached the other end of the tube. The outlet of the tube was held upwards by at least 45°, while the tube was flushed amply (at least 10 times the volume of the sample) with the sample water. The transparent inlet hose was made sure to not have any air bubbles in it, and the aluminium rack was hit with a tool to ensure no air bubbles were left inside the copper tube. The outlet hose was squeezed tight with a tool to increase water pressure in the tube, to decrease possible degassing. The tube was sealed by squeezing the ends of the tube tight with clamps, starting from the outlet clamp. The wall thickness of each tube is 1 mm, and the clamps are designed to squeeze the copper down to 0.7 mm. The inner walls of the Cu-tubes are degreased

for air bubbles to lose their adhesive strength and exit the tube. The Cu-tubes are helium-tight, can stand inner pressure and the samples can be stored for years.

The analysis of the samples was carried out by the Institute of Environmental Physics, University of Bremen, where tritium was separated from water and analysed for ^{3}He and ^{4}He using a sectorfield mass-spectrometer (MAP 2015-50).

Figure 6. Copper tube used in sampling of the noble gases (D-3-17MOS8193). Photo: Kirsti Korkka-Niemi, April 2018.

3.2.2 CFC-12 and SF_6

Chlorofluorocarbons (CFCs) were developed in 1930s for use in e.g. refrigerators and aerosol propellants in place of toxic ammonia and sulfur dioxide, and all CFCs found in environment are of anthropogenic origin (Busenberg and Plummer 1992). CFC-11, CFC-12 and CFC-113 are much used tracers for dating young groundwaters recharged after

their production began; from 1940s to present day (CFC-11 in the 40s, CFC-12 in the 50s, CFC-13 in the 60s) (Plummer and Busenberg 2006). The CFC concentrations in the atmosphere kept rising rapidly until 1990s, when their production was prohibited, and has been declining since. In this study, CFC-12 (CCl_2F_2) was used. Sulfur hexafluoride (SF_6), like CFCs, can be used for tracing groundwaters formed since its production began in the 60s. The SF_6 concentration in the atmosphere is still rising (Darling *et al.* 2010).

The concentration of each gas in a groundwater sample can be matched to the atmospheric concentration of the year the water was recharged, although there are certain complications, such as mixing of waters of water of different ages (Plummer *et al.* 2006). If this is the case, the resulting ages of analysis of different CFCs or SF_6 can be plotted against each other and cross checked with other methods. Presence of CFC-12 in a sample indicates at least a component of the water younger than late 1940s (Plummer *et al.* 1993). CFCs and SF_6 are well-mixed in the atmosphere. Sampling is straightforward, and analysis is time- and cost-effective compared to radio-isotope methods.

Challenges

CFC and SF_6 samples are very vulnerable to contamination during sampling, shipping and processing. Common sources of contamination are contact with even smallest amounts of modern air (bubbles), and pumps, tubing or other equipment containing CFCs (Busenberg and Plummer 1992). For example, lubricants often used in drilling or sampling equipment may degas CFCs for decades (Jürgen Sültenfuß, University of Bremen, Institute of Environmental Physics, personal communication 2019). According to Busenberg and Plummer (1992) and Cook *et al.* (2006), there are many factors affecting the CFC concentrations in groundwater. CFCs tend to microbially degrade in anoxic conditions. As the Viiankiaapa mire is nearby, some of the groundwaters are likely to be anoxic. Some other factors determining the final CFC concentration of water are the thickness of the unsaturated zone, differences in elevation, excess air in the water, contamination by nearby sources, and temperature during recharge.

SF_6 is known to be generated underground (Busenberg and Plummer 2000). For example, Åkesson *et al.* (2015) found SF_6 concentrations in some of their groundwater samples in Sweden to be thousand times higher than their control air samples. Generated SF_6 has also been found in the rapakivi granite regions in Southern Finland (Professor Juha Karhu, University of Helsinki, personal communication 2020).

Sampling

CFC-12 and SF_6 samples were collected in aluminium containers of varying size (Fig. 7), depending on the water output of the well. The sampling procedures were similar to the collection of noble gas samples. The containers were sealed using clamps on each end. The samples were analysed using gas chromatography with electron capture detection at the Bremen Mass Spectrometric Facility, with the accuracy of the analysis being ±0.02 pmol kg^{-1} for CFC-12 and ±0.04 fmol kg^{-1} for SF_6.

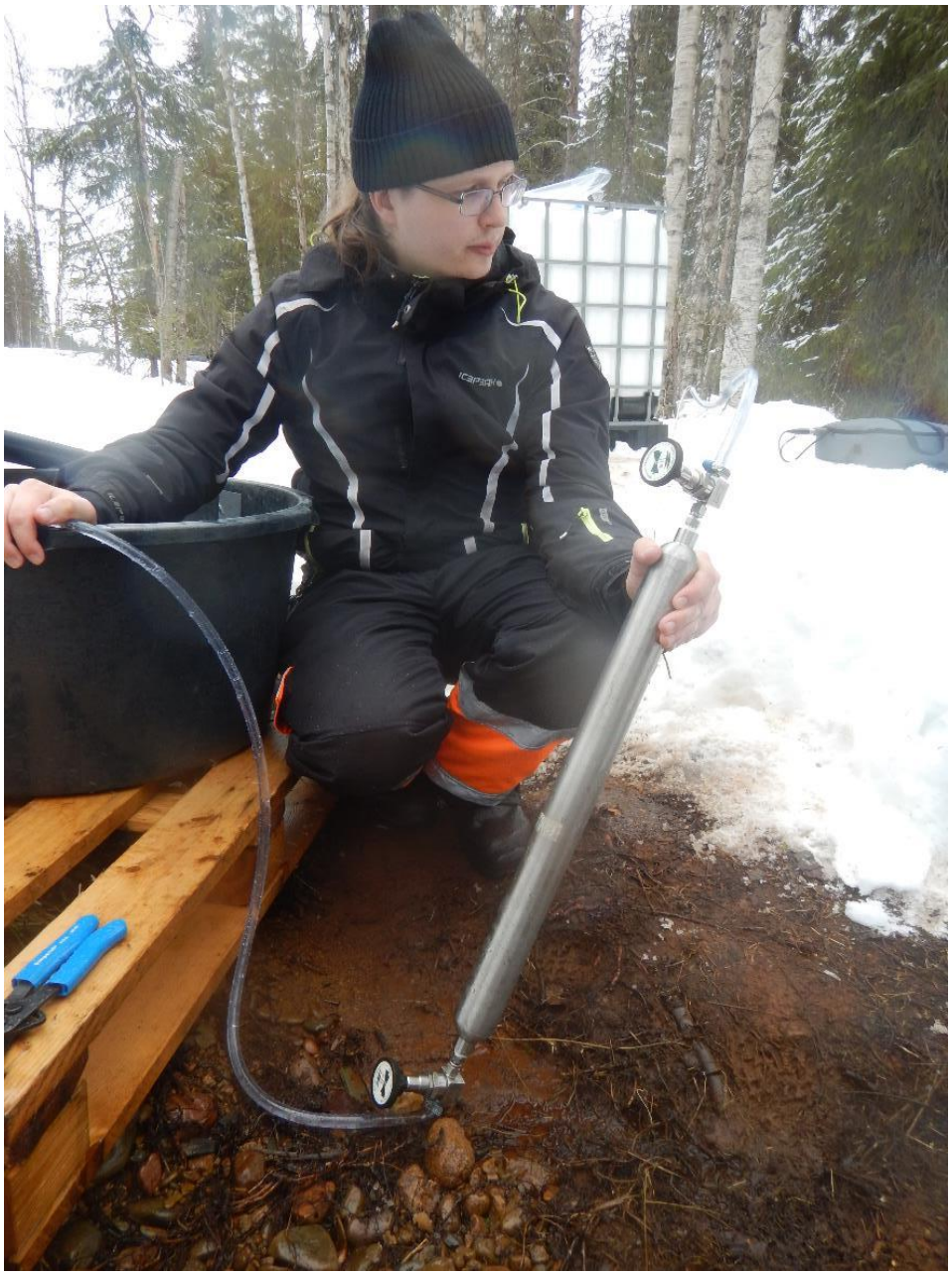

Figure 7. Collecting CFC-12 and SF_6 sample D-3-17MOS8193 in an aluminium container. Photo: Kirsti Korkka-Niemi, April 2018.

3.2.3 ^{14}C

Carbon-14 is well known for its reliable usage for dating groundwater, and other samples. According to Kalin (2000) The radioactive ^{14}C isotope is generated by cosmic rays from atmospheric nitrogen. The ^{14}C atom then forms CO_2 with oxygen and gets mixed with water circulation, and the $^{14}C/^{12}C$ ratio of the water is in equilibrium with atmospheric the ratio. As the water then recharges to form groundwater, it is isolated

from receiving any more ^{14}C from the atmosphere. As the ^{14}C then decays with a half-life of 5 730 years, the amount of ^{14}C left in the water as well as the ratio of ^{14}C and ^{12}C decreases. As the past atmospheric $^{14}C/^{12}C$-ratios can be reconstructed (from e.g. tree rings, lake and marine sediments and glaciers), the $^{14}C/^{12}C$-ratio of a groundwater sample can be measured to determine its time frame of recharge.

Challenges

According to Pearson and Hanshaw (1970) and Thilo and Münnich (1970), groundwater may dissolve carbonate ions from the surrounding rock. As ancient rocks no longer contain ^{14}C, as a result of dissolution the ^{14}C content in the water gets diluted, which leads to too old apparent ages.

Sampling

^{14}C samples were collected in 1 000 ml plastic containers. The bottles were amply spilled through the bottom with sample water, before pouring out some water to leave room for volume change and sealing the bottles. The bottles were then sealed with laboratory film.

The samples were analysed in the laboratory of Curt-Engelhorn-Zentrum Archäometrie GmbH, Germany. The samples were pre-treated using Dissolve-Inorganic-Carbon (DIC) method in a carbonate vacuum-extraction system. The dating was performed using MICADAS-AMS method of the Klaus-Tschira-Archäometrie-Zentrum.

3.3 Field and laboratory measurements

Following parameters were measured at the beginning of the pumping, and at the time of the sampling. In some cases, additional measurements were made during pumping.

- Temperature (YSI 600XL)
- pH (YSI 600XL)
- Electric conductivity (YSI 600XL)
- Water level (Dipper)

- Additional notes, such as colour, smell or pressure
- Some of the samples were titrated *in situ* to find out the $CaCO_3$ content (HACH titrator) using Phenolphthalein and Total Alkalinity method 8203 (DOC316.53.01166). The samples were not warmed up to room temperature, as they were analysed immediately on site.

Figure 8. HAHC titrator used to measure $CaCO_3$ content. May 2018.

Following parameters were analysed at the University of Helsinki, Department of Geosciences and Geography:

- pH was measured with a TitroLine pH meter.
- EC was measured with a CON6/TDS6 conductivity meter (standard SFS 5794).
- Alkalinity was titrated (standard SFS-EN ISO 9963-1).
- Main ion composition was analysed with Metrohm MIC-12 ion chromatography (standards SFS-EN ISO 10304-1 and SFS-EN ISO 14911).

- The stable isotope compositions of hydrogen and oxygen were analysed with a Picarro gas analyser. The accuracy was ≤0.5 ‰ for δ^2H and ≤0.1 ‰ for $\delta^{18}O$.
- Trace element composition was analysed with Agilent 7700 ICP-MS (standard ISO 17294-2). Detection limits are included in Table 8.

3.4 Statistical and graphical methods

The data was examined both statistically and visually using following software and methods. IBM SPSS (25.0.0.1) was used for the statistical analyses, such as analysing data distribution for normality and lognormality, and grouping the samples by attributes using hierarchical clustering. AquaChem 2014.2 (15.204.1025 Waterloo Hydrogeologic) was used to visualize the water types and ion chemistry in piper diagrams. Tables and the boxplot of trace element groups were created with Microsoft Excel (16.0.11929.20436). The maps were created, and the figures as well as some of the tables were enhanced in Clip Studio Paint EX (1.9.5).

4. RESULTS

4.1 Field measurements

The results of field measurements, together with laboratory analysis results for comparison, are presented in Table 2. pH varied between 6.28-9.16, being lowest in the surface water and in the some of the shallow groundwater wells with screen above bedrock surface, and highest in the samples from 12MOS8102 and some of the shallow groundwater wells. Electric conductivity was <0.15 mS cm^{-1} for surface waters and all of the wells with screen above bedrock surface, 0.127-1.338 mS cm^{-1} for the shallow wells with screen below bedrock surface, and 10.2 mS cm^{-1} for the deep D-3-17MOS8193. Alkalinity as $CaCO_3$ was 5-13 mg l^{-1} in surface waters, 34.5-92.5 mS cm^{-1} for the wells with screens above the bedrock surface, 48-173 mS cm^{-1} for the wells with screens

below bedrock surface, and 65 mS cm^{-1} for D-3-17MOS8193. The field measurements of alkality and electric conductivity are in line with laboratory analysis results.

Table 2. Field and laboratory measurements. The alkalinity value calculated from laboratory analysis of ion composition is presented for comparison as well.

		Field measurements				Laboratory	
Sample	Notes	T (°C)	pH	Alk. As $CaCO_3$ (mg/l)	EC (mS/cm)	EC (mS/cm)	Alk. as $CaCO_3$ mg/l calc.
D-3-17MOS8193		7.87	7.58		10.20		65.00
M-1-12MOS8102 23 m		5.10	8.47		0.41		
M-1-12MOS8102 23 m		4.60	8.14		0.35		118.50
M-2-12MOS8102 96 m		5.00	9.16		0.88		116.50
M-4-12MOS8102 65 m		4.20	8.13		0.39		125.50
B-5-GA405 12 m	Dirty water	3.73	7.29		0.24		
B-5B-GA405 12 m		3.91	7.16		0.24		109.00
B-10-17HYD017		4.87	7.47	52	0.13	0.116	48.00
B-11-17HYD013	Black water, smells of hydrogen sulfide	4.50	8.10	80	1.34	1.293	76.50
B-13-17HYD004	Dirty water, clear after 10 l, smells of hydrogen sulfid	4.20	6.79	200	0.36	0.332	173.00
B-14-17HYD006	Clear water at first, then dirty	4.50	7.89	74	0.15	0.155	67.50
B-17-17HYD001	Pressurized, grey, smells of hydrogen sulfide	4.30	8.68	84	0.13	0.142	56.50
G-6-GA305 9 m		3.15	6.55		0.12		92.50
G-8-GA203 4 m	Dirty water	4.00	6.42		0.08		38.00
G-12-17HYD015		3.10	6.61	70	0.14	0.136	69.00
G-15-17HYD016		4.30	7.14		0.07	0.075	34.50
G-18-17HYD003	Dirty water	4.90	8.02		0.14	0.133	59.00
G-19-18HYD033	Dirty water	4.00	6.91		0.04	0.042	28.50
P-20-Rytikuru		4.20	6.28		0.02	0.017	5.50
S-7-Matarakoski		1.54	6.57		0.04		13.00
S-21-Kelukoski		10.60	6.89		0.03	0.028	10.00

4.2 Main ion concentration

The main dissolved ion concentration data is presented in Table 3 and placed into a Piper diagram in Fig. 9. Sample G-19-18HYD033 was left out from the presentations due to a poor ionic balance of 22.5%. This was likely caused by the sample being very muddy, which makes determining alkality difficult. In this case, the assumed approximately correct value could still be calculated based on the ion composition, but the sample was dismissed, nonetheless.

Most of the shallow groundwater wells with screens above and below bedrock surface were of Calcium bicarbonate or Magnesium bicarbonate type, except for B-11, which had much more SO_4 and Cl. The samples from the deep 18MOS8193 were of sodium sulphate type. The ion compositions of the samples M-1, M-2 and M-4 from the 12MOS8102 were scattered between the previous two groups.

The total dissolved solids (TDS) was 20-40 mg l^{-1} for surface waters, 98-238 mg l^{-1} for shallow wells with screens above bedrock surface, and 136-465 mg l^{-1} for wells with

screens below bedrock surface, except for B-11-17HYD013, which had 905 mg l^{-1}. The 12MOS8102 had 429-690 mg l^{-1} of TDS, and the deep 17MOS8193 had 7680-8739 mg l^{-1}, about ten times more than any other well.

Table 3. Results of the ion chemical analyses. $CaCO_3$ and HCO3 values are calculated based on alkalinity.

	Cations mg/l					Anions mg/l						Calc.	Calc.			Ionic sum meq/l		
	Na	K	Ca	Mg	pH (lab)	F	Cl	NO_3	PO_4	SO_4	Alk. mmol/l	Alk. as $CaCO_3$ mg/l	HCO_3 mg/l	TDS mg/l	Water type	∑Cations	∑Anions	IB%
D-22-17MOS8193-140418	1824.25	50.75	632.25	279.25	7.66	0.50	2592.00	5.25	0.00	3211.25	1.30	65.00	79.30	8739.80	Sodium chloride	135.18	141.39	2.24
D-3-17MOS8193	1609.00	56.25	592.25	264.50	7.83	0.75	2132.75	9.75	0.00	3260.00	1.30	65.00	79.30	8069.55	Sodium sulphate	122.75	129.53	2.69
D-23-17MOS8193-210418	1614.25	55.75	607.00	269.25	7.87	0.75	2125.75	10.75	0.00	3256.50	1.29	64.50	78.69	8083.19	Sodium sulphate	124.09	129.27	2.04
D-24-17MOS8193-270418	1509.00	53.00	582.50	259.25	7.94	0.50	1954.00	10.25	0.00	3257.75	1.29	64.50	78.69	7769.44	Sodium sulphate	117.40	124.43	2.91
D-9-17MOS8193-29A	1511.75	49.25	590.50	261.75	7.95	0.25	1897.00	7.50	0.00	3237.25	1.29	64.50	78.69	7698.44	Sodium sulphate	118.03	122.34	1.79
D-25-17MOS8193-29B	1476.25	55.25	581.00	257.00	7.98	0.50	1905.50	10.00	0.00	3252.25	1.29	64.50	78.69	7680.94	Sodium sulphate	115.77	122.94	3.00
M-1-12MOS8102 23 m	59.38	6.62	41.42	22.25	7.86	0.16	113.16	0.22	0.00	47.67	2.37	118.50	144.57	553.95	Bicarbonate	6.65	6.57	0.63
M-2-12MOS8102 96 m	71.42	7.25	65.64	20.66	8.11	0.21	48.21	0.23	0.00	217.89	2.33	116.50	142.13	690.14	Mixed	8.27	8.24	0.16
M-4-12MOS8102 65 m	39.86	4.82	29.74	9.61	8.11	0.18	17.18	0.23	0.00	49.50	2.51	125.50	153.11	429.73	Bicarbonate	4.13	4.04	1.15
B-5B-GA405 12 m	2.11	1.15	24.85	11.53	7.26	0.07	2.80	0.27	0.00	4.39	2.18	109.00	132.98	289.15	Calcium bicarbonate	2.31	2.36	1.04
B-10-17HYD017	2.90	1.26	13.52	3.07	7.30	0.08	1.22	0.00	0.00	7.97	0.96	48.00	58.56	136.58	Calcium bicarbonate	1.09	1.16	3.53
B-11-17HYD013	66.45	2.91	110.83	51.19	7.94	0.16	244.82	0.00	0.00	259.19	1.53	76.50	93.33	905.37	Mixed	12.71	13.84	4.27
B-13-17HYD004	2.52	1.29	67.46	7.97	6.98	0.08	1.24	0.00	0.00	0.74	3.46	173.00	211.06	465.35	Calcium bicarbonate	4.16	3.51	8.46
B-14-17HYD006	1.77	1.18	22.35	3.61	7.79	0.03	2.03	1.52	0.00	6.08	1.35	67.50	82.35	188.41	Calcium bicarbonate	1.52	1.56	1.32
B-17-17HYD001	2.95	3.07	18.67	2.46	8.27	0.08	1.12	<0.1	0.00	10.57	1.13	56.50	68.93	164.36	Calcium bicarbonate	1.34	1.39	1.70
G-6-GA305 9 m	1.91	0.93	16.53	11.91	6.97	0.05	0.81	<0.1	0.00	0.51	1.85	92.50	112.85	237.99	Magnesium bicarbonate	1.91	1.89	0.66
G-8-GA203 4 m	1.62	0.56	6.64	4.96	6.65	0.03	0.79	0.33	0.00	1.25	0.76	38.00	46.36	100.55	Bicarbonate	0.82	0.82	0.57
G-12-17HYD015	2.25	0.73	11.14	8.48	6.85	0.07	1.16	<0.1	0.00	1.52	1.38	69.00	84.18	178.52	Magnesium bicarbonate	1.37	1.45	2.75
G-15-17HYD016	1.85	1.94	9.66	3.58	6.84	0.06	1.57	0.93	0.00	2.56	0.69	34.50	42.09	98.74	Calcium bicarbonate	0.91	0.81	5.92
G-18-17HYD003	2.11	2.25	19.41	3.37	7.43	0.06	1.15	0.00	0.00	9.26	1.18	59.00	71.98	168.58	Calcium bicarbonate	1.40	1.41	0.46
G-19-18HYD033	1.99	5.40	10.33	3.69	6.80	0.04	1.03	0.00	0.00	2.84	0.57	28.50	34.77	88.59		1.04	0.66	22.50
P-20-Rytikuru	1.09	0.67	2.03	0.65	5.96	0.02	1.00	0.00	0.11	2.29	0.11	5.50	6.71	20.06	Bicarbonate	0.22	0.19	7.20
S-7-Matarakoski	1.44	0.47	3.78	1.31	6.65	0.07	0.83	0.45	0.00	2.63	0.26	13.00	15.86	39.83	Calcium bicarbonate	0.37	0.35	3.14
S-21-Kelukoski	0.80	0.52	2.88	1.00	6.49	0.03	1.01	<0.1	0.05	2.34	0.20	10.00	12.20	30.83	Calcium bicarbonate	0.27	0.28	1.12

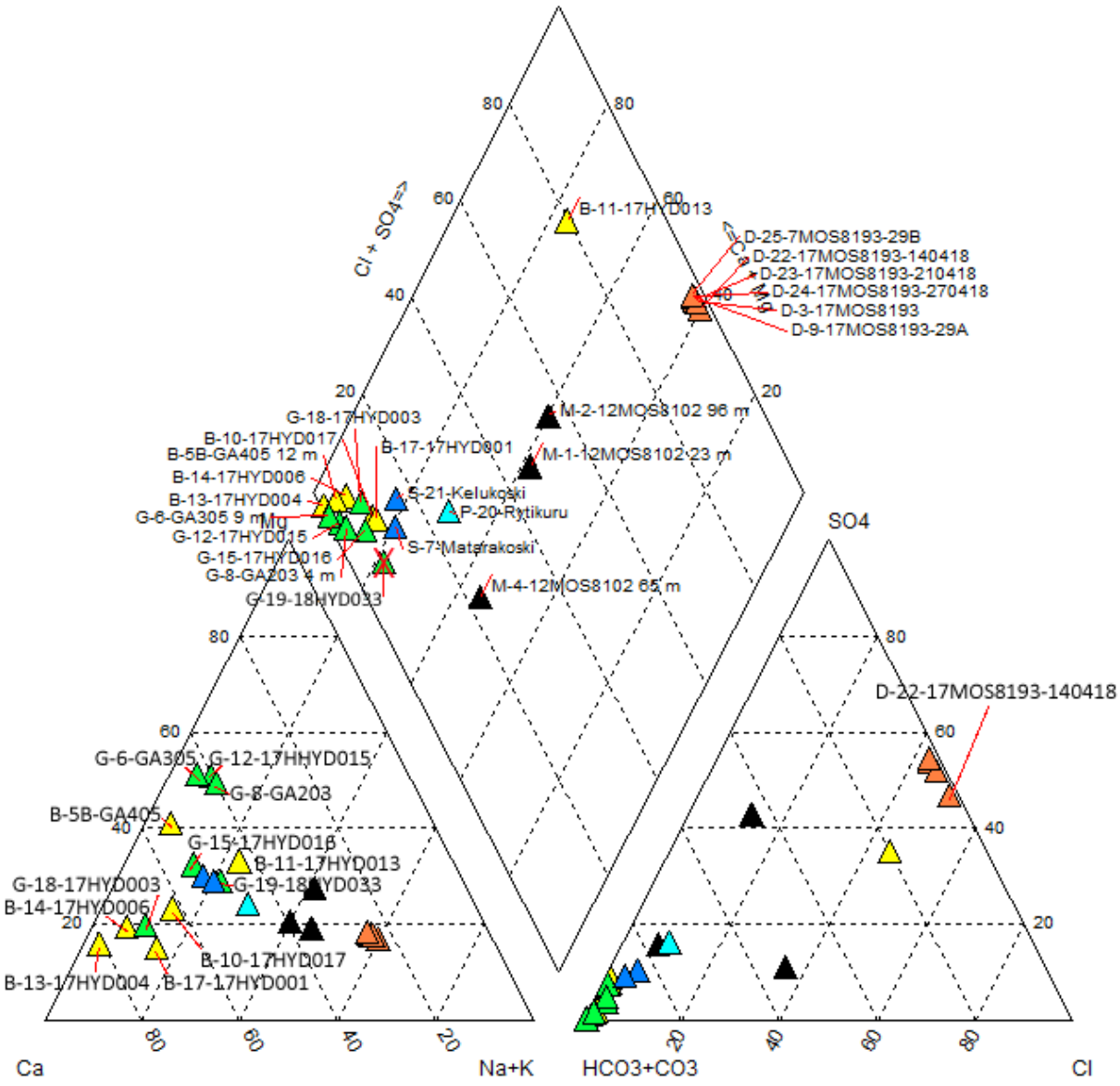

Figure 9. Piper diagram of the ion chemistry of the samples. Symbol colors as in Fig. 4. AquaChem 2014.2 (15.204.1025).

4.3 δ^2H and $\delta^{18}O$ values of water

The δ^2H and $\delta^{18}O$ data is presented in Table 4. δ^2H varies between -111.5 and -90.2, $\delta^{18}O$ between -15.19 and -12.06, and D-excess between 4.1 and 10.3. The analytical data for δ^2H and $\delta^{18}O$ (Table 4) is presented in Fig. 10 in relation to the Local Meteoric Water Line (LMWL) (Kortelainen 2007) and Global Meteoric Water Line (GMWL) (Graig 1961). Majority of the samples are located below the LMWL and GMWL forming two separate groups. One group is located in the lower left corner of the diagram and falls in the vicinity of the composition of the mean annual precipitation in the Sodankylä area, relatively close to the LMWL and GMWL. Another group is located in the upper right corner of the diagram, clearly displaced down from the LMWL and GMWL.

Table 4. Results of the δ^2H and $\delta^{18}O$ analyses.

	δ^2H (‰, VSMOW)	$\delta^{18}O$ (‰, VSMOW)	D-excess (‰)
D-3-17MOS8193	-108.7	-14.61	8.2
D-9-17MOS8193-29A	-109.1	-14.70	8.5
M-1-12MOS8102 23 m	-98.2	-12.88	4.8
M-2-12MOS8102 96 m	-100.7	-13.18	4.7
M-4-12MOS8102 65 m	-99.2	-12.91	4.1
B-5B-GA405 12 m	-95.7	-12.50	4.3
B-10-17HYD017	-111.1	-14.99	8.8
B-11-17HYD013	-107.5	-14.54	8.8
B-13-17HYD004	-94.0	-12.48	5.9
B-14-17HYD006	-104.7	-14.08	7.9
B-17-17HYD001	-111.5	-15.19	10.0
G-6-GA305 9 m	-94.6	-12.40	4.7
G-8-GA203 4 m	-94.6	-12.41	4.7
G-12-17HYD015	-90.2	-12.06	6.3
G-15-17HYD016	-107.9	-14.49	8.0
G-18-17HYD003	-110.0	-15.04	10.3
G-19-18HYD033	-108.9	-14.73	9.0
P-20-Rytikuru	-107.9	-14.69	9.6
S-7-Matarakoski	-97.5	-12.99	6.5
S-21-Kelukoski	-112.2	-15.08	8.5

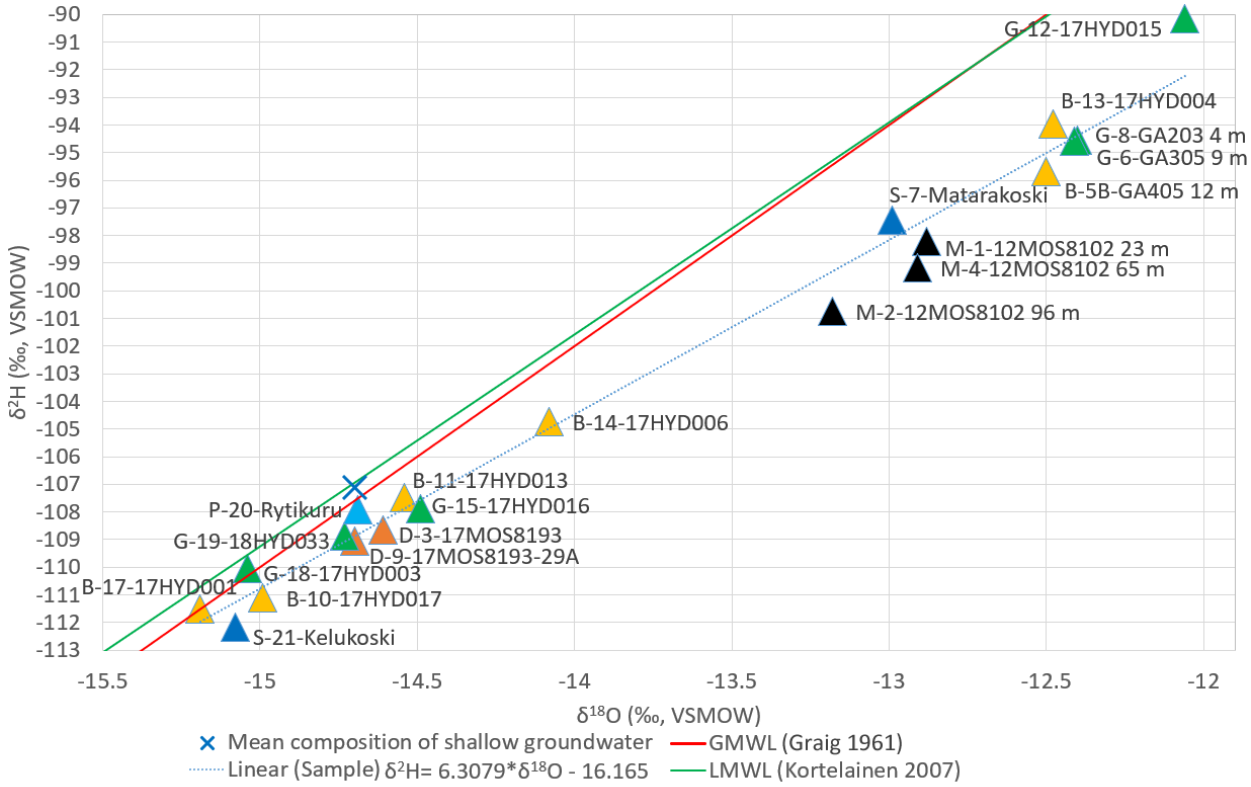

Figure 10. δ^2H and $\delta^{18}O$ in relation to the global and local meteoric water lines. The mean composition of shallow groundwaters is from Siurunmaa, Sodankylä according to Kortelainen (2007). Symbol colors as in Fig. 4.

The two surface water samples from the River Kitinen, S-7 and S-21, show a clear difference in their isotope ratios. Sample S-7 was collected in April, whereas Sample S-21 was collected one month later during spring flooding. Evidently, snowmelt during spring flooding has a major effect on the composition of the river water at that time.

The samples D-3 and D-9 from borehole 17MOS8193 fall on the δ^2H and $\delta^{18}O$ diagram relatively close to composition of the mean annual precipitation in the area. In contrast, the samples M-1, M-2 and M-4 from the adjacent borehole 12MOS8102 are clearly displaced from the composition of the mean annual precipitation and fall below the LMWL and GMWL. The samples were taken from three different depths (23, 65 and 96 m) in fractured upper part of bedrock. Also samples B-5B-GA405, G-6-GA305 and G-8-GA203 represent a water type, which is distinct in composition compared to that of the mean annual precipitation.

4.4 Radiocarbon

Table 5. Radiocarbon data for the three samples ('Age cal' calibrated with Oxcal, Intcal13 95.4 %).

	^{14}C lab no.	Date (^{14}C, BP)	+ -	Age cal (BP, 2-sigma range)
D-3-17MOS8193	36436	30210	130	33940-34560
D-9-17MOS8193-29A	36438	28200	110	31560-32540
M-4-12MOS8102 65 m	36437	3295	24	3580-3460

Two samples from borehole 17MOS8193 and one from borehole 12MOS8102 were analysed for the content of ^{14}C. After calibration by Oxcal using the Intcal13 calibration curve (Reimer *et al.* 2013), both ^{14}C samples from borehole 17MOS8193 yielded apparent ages of ~32 ka (Table 5). The ^{14}C concentrations in these samples are very low and therefore suspect to have been resulted from contamination during sampling.

The water from the depth of 65 m in the adjacent well 12MOS8102 yielded a calibrated apparent radiocarbon age of about 3500 a. The age refers to dissolved inorganic carbon in water, which is not necessarily the same as the age of the water. In prolonged contact with mineral matter on the fracture walls, the water may have dissolved unspecified quantities of radiocarbon-free ancient carbonate minerals from bedrock fractures, increasing the apparent ^{14}C age (Pearson and Hanshaw 1970).

4.5 T/He

Thirteen water samples were collected for recharge dating using the ^{3}H/^{3}He method. Some of the samples were analysed multiple times. The analytical results are presented in Table 6. Underground generation of helium made age determination of the samples M-1, M-2 and M-4 from 12MOS8102 and B-11-17HYD013 not possible, but they contained 1.42-2.95 TU of tritium. No tritium and thus young groundwater component was found in 17MOS8193. Shallow groundwater wells had tritium contents of 0.32-6.46, and were dated to have recharged in 1973-1985, but B-10-17HYD017 was dated to 1955 and B-14-17HYD006 to 2018.

Table 6. Concentrations of ^{3}H, ^{3}He, ^{4}He, and the contents of tritiogenic ^{3}He and the initial ^{3}H, with derived age data.

	Tritium (TU)	n	^{3}He (ccSTP/kg)	n	^{4}He (ccSTP/kg)	n	Tritiogenic 3He (TU)	n	Initial tritium (TU)	n	T/He age	n
D-3-17MOS8193	0.00	2	6.29E-09	2	1.16E-01	2					<1950	2
D-9-17MOS8193-29A	0.00	2	6.50E-09	2	1.12E-01	2					<1950	2
M-1-12MOS8102 23 m	2.95	2	5.25E-10	2	4.61E-03	2						
M-2-12MOS8102 96 m	1.42	2										
M-4-12MOS8102 65 m	1.81	2	5.29E-10	2	5.67E-03	2						
B-5-GA405 12 m	4.87	2	2.32E-10	2	9.71E-05	2	58.7	2	63.6	2	1973	2
B-5B-GA405 12 m	6.46	4	2.11E-10	4	9.60E-05	4	51.1	4	57.5	4	1979	4
B-10-17HYD017	0.32	4	1.10E-10	4	1.05E-04	4	10.9	4	11.2	4	1955	4
B-11-17HYD013	1.49	1	4.31E-09	1	7.14E-02	1						
B-13-17HYD004	4.82	1	1.60E-10	1	2.45E-04	1	35.1	1	39.9	1	1981	1
B-14-17HYD006	6.39	2	8.13E-11	2	8.51E-05	2	0.0	2			2018	2
B-17-17HYD001	4.46	4	1.53E-10	4	2.18E-04	4	30.0	4	34.4	4	1982	4
G-6-GA305 9 m	5.79	2	1.60E-10	2	8.41E-05	2	32.9	2	38.7	2	1985	2

4.6 CFC-12 and SF_6

Nine CFC-12 and SF_6 sample sets were collected for recharge dating (Table 7). The sample M-2-12MOS8102 was rejected due to poor sampling conditions and B-10-17HYD017 due to a leakage during shipping. The CFC-12 result of D-3-17MOS8193 was deemed contaminated due to the sample D-9 showing CFC-12 content much more reasonable in light of other methods.

The sample D-9-17MOS8193 had 0.08 pmol kg^{-1} of CFC-12, while all other samples had 0.24-0.86 pmol kg^{-1}. Both samples from 17MOS8193 had 0.14-0.15 fmol kg^{-1} of SF_6, while all other samples had 2.15-4.17 fmol kg^{-1}.

Table 7. CFC-12 and SF6 concentrations.

	SF_6 +-0.04 fmol/kg	CFC-12 +-0.02 pmol/kg
D-3-17MOS8193	0.15	1.63
D-9-17MOS8193-29A	0.14	0.08
M-1-12MOS8102 23 m	2.35	0.58
M-4-12MOS8102 65 m	2.15	0.35
B-5B-GA405 12 m	2.80	0.40
B-11-17HYD013	4.17	0.86
G-6-GA305 9 m	2.34	0.24

4.7 Trace elements

The trace element analysis results are presented in Table 8. The river water sample S-21 had 6.47 ppb of U, over six time more than any other sample. During years of continuous monitoring, the uranium content of the water has not exceeded 0.06 ppb (Anne Rautio, AA Sakatti Mining Oy, personal communication 2020), so the result is likely erroneous.

Contents of most trace elements vary by orders of magnitude. Highest concentrations of most elements (Al, Si, P, V, Cr, Mn, Fe, Co, As and Se) in groundwaters were found in certain shallow wells with screens below bedrock surface, except Ni, Zn and Pb, which had highest concentrations in 12MOS8102, and Mo and Cd, which were highest in two of the shallow wells with screen over bedrock surface, G-15-17HYD016 and G-19-18HYD033.

B-13-17HYD004 had exceptionally high contents of Si, P, V, Cr, Mn, Fe, Co and As. B-5, B-5B-GA045 and B-10-17HYD017 were the other shallow groundwater wells to have high Si, P and Fe contents Zn in well GA405 rose from 1.08 to 50.26 ppb as the well was resampled due to poor refill rate (samples B-5 and B-5B). The samples with the generally lowest trace element contents were G-8-GA203, G-12-17HYD015 and the river samples S-7 and S-21.

Table 8. The results of the trace element analysis. All elements are measured in ppb. The red bars represent the amount of the element in the sample in proportion to the other samples.

	27 Al	28 Si	31 P	51 V	52 Cr	55 Mn	56 Fe	59 Co	60 Ni	63 Cu	66 Zn	75 As	78 Se	95 Mo	111 Cd	208 Pb	238 U
	ppb	ppm	ppb	ppb	ppb	ppb	ppb	ppb	ppb	ppb	ppb	ppb	ppb	ppb	ppb	ppb	ppb
Detection limit	<1.100	<0.020	<4.400	<0.030	<0.040	<0.080	<1.100	<0.010	<0.030	<0.100	<0.100	<0.020	<0.040	<0.030	<0.006	<0.030	<0.009
D-22-17MOS8193-1404	12.67	8.78	29.15	0.13	0.25	200.63	334.08	0.03	0.19	<0.100	2.57	0.31	<0.040	11.24	0.02	<0.030	0.99
D-3-17MOS8193	27.30	9.12	27.39	0.09	0.08	182.40	289.08	0.02	0.12	<0.100	2.33	0.27	<0.040	10.29	0.01	<0.030	0.82
D-23-17MOS8193-2104	16.35	8.88	9.99	0.09	0.50	179.41	282.34	0.02	0.15	0.19	2.90	0.26	<0.040	10.22	0.01	<0.030	0.79
D-24-17MOS8193-2704	31.26	8.91	7.29	0.09	0.46	173.09	271.48	0.02	0.14	<0.100	1.80	0.25	<0.040	9.84	0.01	<0.030	0.74
D-9-17MOS8193-29A	24.46	8.96	10.28	0.08	0.06	171.95	259.36	0.02	0.10	<0.100	1.41	0.25	<0.040	9.82	0.01	<0.030	0.76
D-25-17MOS8193-29B	27.59	9.13	9.47	0.08	0.09	175.02	261.79	0.02	0.12	<0.100	1.38	0.25	<0.040	9.70	0.01	<0.030	0.74
M-1-12MOS8102 23 m	23.07	2.35	8.44	<0.030	0.28	241.54	698.86	0.26	37.17	2.05	161.84	0.15	<0.040	13.40	0.02	<0.030	<0.009
M-2-12MOS8102 96 m	44.43	2.93	21.72	0.04	0.28	148.39	158.89	0.04	2.21	2.30	229.60	0.45	<0.040	3.36	0.01	0.05	0.16
M-4-12MOS8102 65 m	34.75	3.06	15.68	<0.030	0.10	146.06	853.26	0.07	0.29	<0.100	125.60	0.66	<0.040	4.53	0.01	<0.030	0.04
B-5-GA405 12 m	15.07	9.00	122.62	0.37	0.73	242.06	10311.63	0.21	0.37	<0.100	1.08	2.07	<0.040	0.19	<0.006	<0.030	<0.009
B-5B-GA405 12 m	19.45	9.10	103.26	0.37	0.71	236.22	10234.30	0.23	0.55	<0.100	50.26	1.82	<0.040	0.18	<0.006	<0.030	0.01
B-10-17HYD017	24.73	10.27	96.92	0.03	0.10	221.89	4990.31	<0.010	0.10	<0.100	0.36	1.45	<0.040	0.24	<0.006	<0.030	<0.009
B-11-17HYD013	23.15	5.15	17.43	0.03	0.08	612.16	1310.37	0.05	0.12	<0.100	1.31	0.47	<0.040	1.39	<0.006	<0.030	1.03
B-13-17HYD004	25.53	10.61	82.52	2.20	5.75	1088.99	13660.22	2.45	0.88	<0.100	0.50	21.93	<0.040	0.22	<0.006	<0.030	0.13
B-14-17HYD006	29.88	4.85	12.11	0.15	0.54	8.53	15.88	0.13	1.79	<0.100	0.47	0.07	0.29	0.15	<0.006	<0.030	<0.009
B-17-17HYD001	240.12	6.00	11.32	2.35	0.35	40.10	15.65	0.03	0.15	<0.100	<0.100	0.49	0.26	1.44	<0.006	<0.030	0.04
G-6-GA305 9 m	17.26	7.41	5.82	0.07	0.70	196.89	279.70	1.44	3.04	1.55	92.30	0.09	<0.040	0.05	0.03	<0.030	0.08
G-8-GA203 4 m	18.14	4.45	19.05	0.05	0.14	1.06	11.15	0.10	0.34	0.19	1.81	0.03	<0.040	<0.030	<0.006	<0.030	0.02
G-12-17HYD015	28.44	6.88	17.99	0.33	1.06	3.33	2.23	0.06	4.92	0.47	1.84	0.03	<0.040	0.57	<0.006	<0.030	0.01
G-15-17HYD016	27.42	4.83	12.11	0.31	0.31	16.49	6.61	0.10	1.33	0.63	4.22	0.10	0.11	33.03	0.04	<0.030	<0.009
G-18-17HYD003	25.99	7.14	70.20	0.27	0.04	109.76	562.75	0.07	0.19	0.24	1.11	1.32	<0.040	0.44	0.04	<0.030	0.29
G-19-18HYD033	44.31	4.84	24.88	0.65	0.21	182.72	58.89	1.61	2.45	0.13	0.68	0.08	0.09	28.13	0.03	<0.030	<0.009
P-20-Rytikuru	124.94	4.18	24.44	0.17	0.36	2.76	36.44	0.24	0.95	3.41	1.08	0.02	0.08	0.12	<0.006	<0.030	<0.009
S-7-Matarakoski	33.23	2.35	21.68	0.13	0.29	32.38	474.28	0.08	0.25	<0.100	0.73	0.10	<0.040	0.16	<0.006	<0.030	0.02
S-21-Kelukoski	32.47	1.33	13.92	0.08	0.34	9.26	277.76	0.04	0.47	<0.100	0.66	0.12	<0.040	0.06	<0.006	<0.030	6.47

5. DISCUSSION

5.1 Ion composition

The ion composition shows division of most of the samples into two very distinct water types, and the rest of the samples falling in between (Fig. 11). The first dominating water type consists of the most surficial groundwaters in the shallow wells with screens above and below bedrock surface. The ionic composition in these wells were largely similar, and typical for relatively recently permeated rainwater (Blomqvist 1999), although the wells with screen below bedrock level tended to have a higher Ca/Mg ratio, possibly showing the beginning of the geochemical groundwater evolution. All the samples from 17MOS8193, being the deepest samples, represent the other distinct water type group. Their compositions were very similar to each other, being somewhat on the point between Na-Cl and Na-SO_4 waters. The TDS varies from 7680 to 8740 mg l^{-1}, being much more saline than the other samples, typical for wells of this depth (Blomqvist 1999), although about half less than the salinity of Outokumpu Deep Drill Hole R2500 at depth of 1 000 m. The main ion compositions are also presented as stiff diagrams in Fig. 12.

Most of the other samples end up between these two groups. Due to the lack of samples between the two end members, the evolution of these waters seems to be mostly controlled by mixing of the two, rather than geochemical evolution. The samples from the River Kitinen had a component with increased Na, K, SO_4 and Cl contents compared to the shallow groundwaters. This could indicate some discharge of bedrock groundwater component in the river, but determining the source for certain would require further studying. The Rytikuru spring sample had an even larger content of Na, K, SO_4 and Cl, and the samples M-1, M-2 and M-4 from 12MOS8102 were about halfway between the waters from shallow wells and the deep 17MOS8193, which supports the

other methods indicating a mixture of young and old groundwater in the well. They were rather scattered in their HCO_3+CO_3-SO_4-Cl ratios, much more so than the other samples.

B-11-17HYD013 is the only sample very different from any other, containing much more Cl and SO_4. To find out the reason for the distinct composition would require further studies, as the cause could be either geogenic, anthropogenic or of some other source.

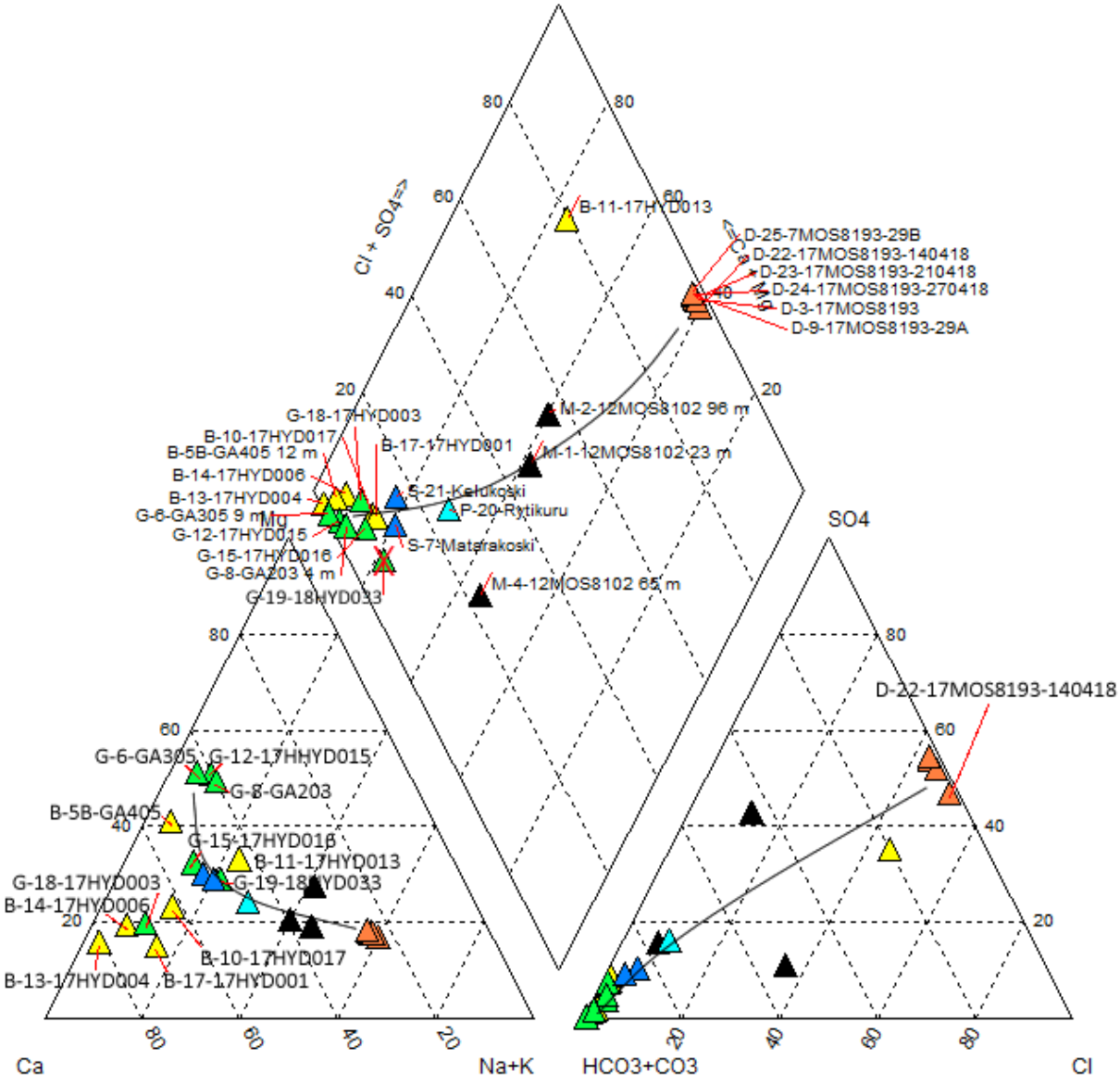

Figure 11. A piper diagram of the samples, with a trendline of waters formed by either groundwater evolution or mixing of young and old groundwaters. Sample colors by sample type as in Fig. 4. AquaChem 2014.2 (15.204.1025).

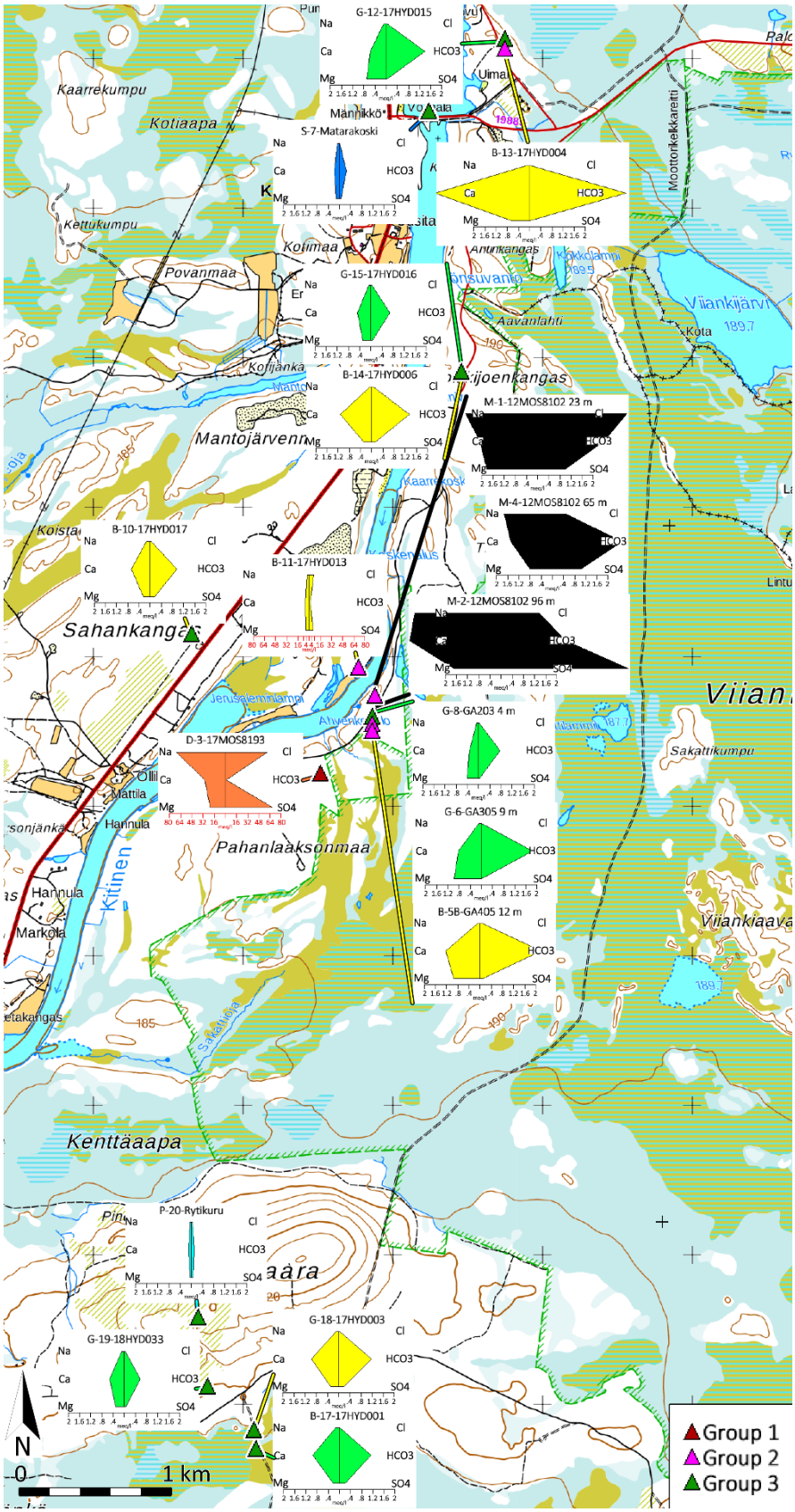

Figure 12. Stiff diagrams of each groundwater well. Note the scale of 0–80 meq l^{-1} for samples D-3 and B-11, and 0–2 meq l^{-1} for the rest of the samples. The samples were divided into groups by the contents of main ions (Table 3). Stiff diagram colors by sample type as in Fig. 4.

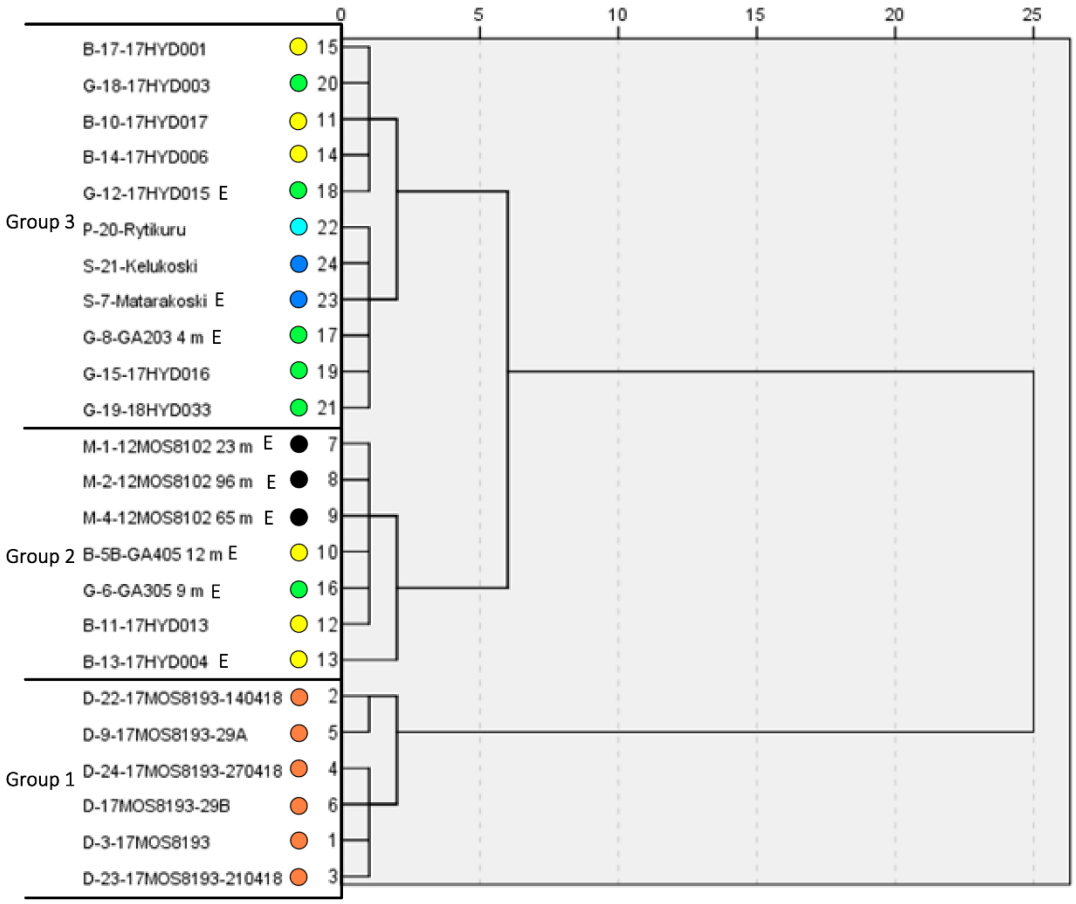

Figure 13. Dendrogram based on the main ion composition of the samples using hierarchical clustering (Ward linkage, Euclidean distance, standardized range 0 to 1). Samples interpreted to have been affected by evaporation (based on δ^2H and $\delta^{18}O$) are marked with a letter E. Symbol colors as in Fig. 4. SPSS 25.0.0.1.

Cluster analysis was applied to divide the water samples into three distinct groups using the concentrations of main dissolved components (Na, K, Ca, Mg, F, Cl, NO_3, PO_4, SO_4, $CaCO_3$, HCO_3) as variables (Fig. 13). Trace element concentrations were not included, as they increased the complexity of the interpretation, most probably resulting from local geochemical variability in bedrock. These groups are discussed in more detail in Chapter 5.5.

- Group 1. The deep brackish groundwaters from borehole 17MOS8139 are chemically distinct from all other waters and form a group of their own. The samples belonging to this group are D-3, -9, -22, -23, -24 and -25.
- Group 2. The second group includes groundwater samples from relatively shallow bedrock boreholes (<250m), and one sample from a shallow groundwater well. The group includes water samples M1, -2 and -4 from borehole 12MOS8102 and other borehole samples B-5B-GA405, B-11-17HYD013 and B-13-17HYD004, all located in the fractured upper part of the bedrock, as well as a shallow groundwater well sample G-6-GA305.
- Group 3. The samples in Group 3 show large similarities in their chemical composition. They include two river water samples, five shallow groundwater samples from the sedimentary cover as well as three water samples from shallow bedrock boreholes. The samples included are S-7, S-21, P-20, B-10-17HYD017, B-14-17HYD006, B-17-17HYD001, G-8-GA203, G-12-17HYD015, G-15-17HYD016, G-18-17HYD003 and G-19-18HYD033. Some of the samples have been collected from wells or boreholes located close to the River Kitinen, whereas others are located at distances over 1 km.

5.2 δ^2H and δ^{18}O

Groundwater recharge can be derived either directly from precipitation, characterized by δ^2H and δ^{18}O values falling close to the global meteoric water line or indirectly from surface water, which has been stored in open surface water bodies (Gat and Tzur 1967, Gonfiantini 1986). The δ^2H and δ^{18}O values of the latter water type are isotopically modified by evaporation (Friedman 1953). As a result of evaporation, the δ^2H and δ^{18}O values of remaining water increase and are shifted down from the GMWL.

Based on the data from shallow groundwaters, the mean annual δ^2H and δ^{18}O values of precipitation at the Sodankylä area have been determined by Kortelainen (2007) to be -107.1 and -14.7 ‰, respectively (Fig. 10, Fig. 14). In addition, monthly isotope values have seasonal variation, which for the Rovaniemi precipitation station has been measured to be 66 ‰ for δ^2H and 9 ‰ for δ^{18}O (Kortelainen, 2007). This variation is

largely averaged in groundwaters, which in Finland approximate the δ^2H and $\delta^{18}O$ values of the mean annual precipitation (Kortelainen and Karhu, 2004).

On the δ^2H - $\delta^{18}O$ diagram, the evaporated waters form an evaporation trend, with a starting point at the local mean annual precipitation. The evaporation trend can be clearly observed in the δ^2H and $\delta^{18}O$ data of this study (Fig. 10, Fig. 14).

Two distinct evaporated surface water types can be distinguished in the Sakatti area. The first one is represented by the water of the River Kitinen. Two analyses for the river water are included in this study. The isotopic composition of the sample S-7 from Matarakoski is distinctively displaced from the meteoric water line and lies on the evaporation line. The composition may reflect evaporation in the Porttipahta reservoir or in the smaller open water pools in the mire area. The other water sample from the River Kitinen, Kelukoski S-21, plots on the δ^2H - $\delta^{18}O$ diagram close to the GMWL, and it has δ^2H and $\delta^{18}O$ values even lower than those in the mean annual precipitation. Based on the sampling date, it represents the composition of river water during spring flooding, and the water likely is largely composed of snowmelt derived from winter precipitation (Kortelainen 2007).

The most potential source water type for infiltration with an evaporated isotope signal is derived from the surface water pools in the surrounding mire areas, due to the groundwater flow gradient being clear from the mire towards the River Kitinen (Åberg *et al.* 2019a). The evaporated δ^2H and $\delta^{18}O$ signal in this water type at Sakatti has been documented by Lahtinen (2017, Salonen *et al.* 2015, Bigler 2018, Åberg *et al.* 2019a), who analysed water samples collected from the pools and from the Sakattioja ditch moving water from the mire area.

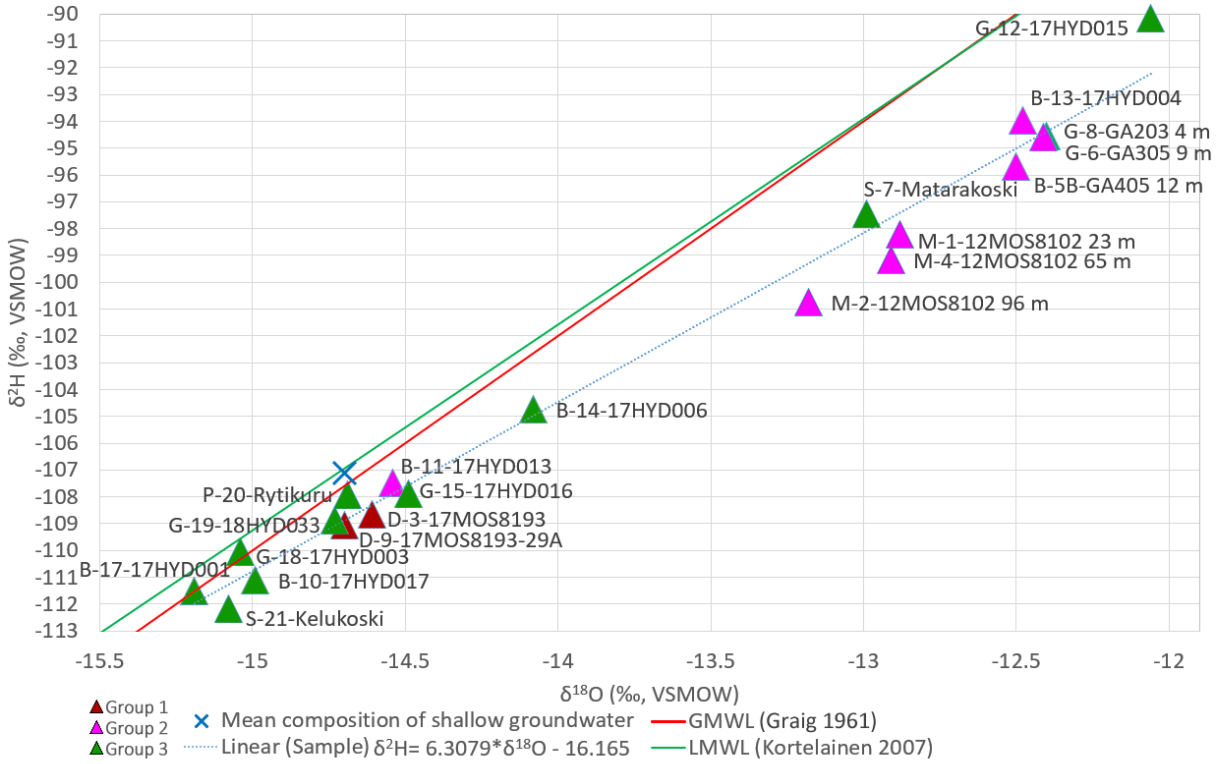

Figure 14. δ^2H and $\delta^{18}O$ of the water samples shown for groups formed on the basis of main ion contents. The mean annual composition of shallow groundwater is from Siurunmaa, Sodankylä (Kortelainen 2007).

5.3 Tritium

In radioactive decay, one atom of ^3H forms one atom of ^3He, and therefore the initial ^3H contents of the groundwater at the time of its recharge can be calculated by summing the contents of tritiogenic ^3He with that of remaining ^3H (Healy 2010). As with other tracers, it is assumed that the water mass has been closed relative to ^3H and ^3He. The contents of calculated initial ^3H are in Fig. 15 compared to measurements of ^3H in northern hemisphere precipitation from three precipitation stations (International Atomic Energy Agency/World Meteorological Organization, 2019). The calculated initial ^3H concentrations fall along the trend formed by the ^3H contents in precipitation at the time of the calculated recharge, suggesting that no significant gain or loss of ^3H or ^3He has occurred. The infiltration of the sample B-11-17HYD013 appears to predate the maximum peak at 1960-1970, and the groundwater samples dated to 1970-1990 show

a decreasing trend in their initial ^{3}H concentrations similar to that in the ^{3}H values of precipitation. This pattern gives independent support to the accuracy of the T/He data.

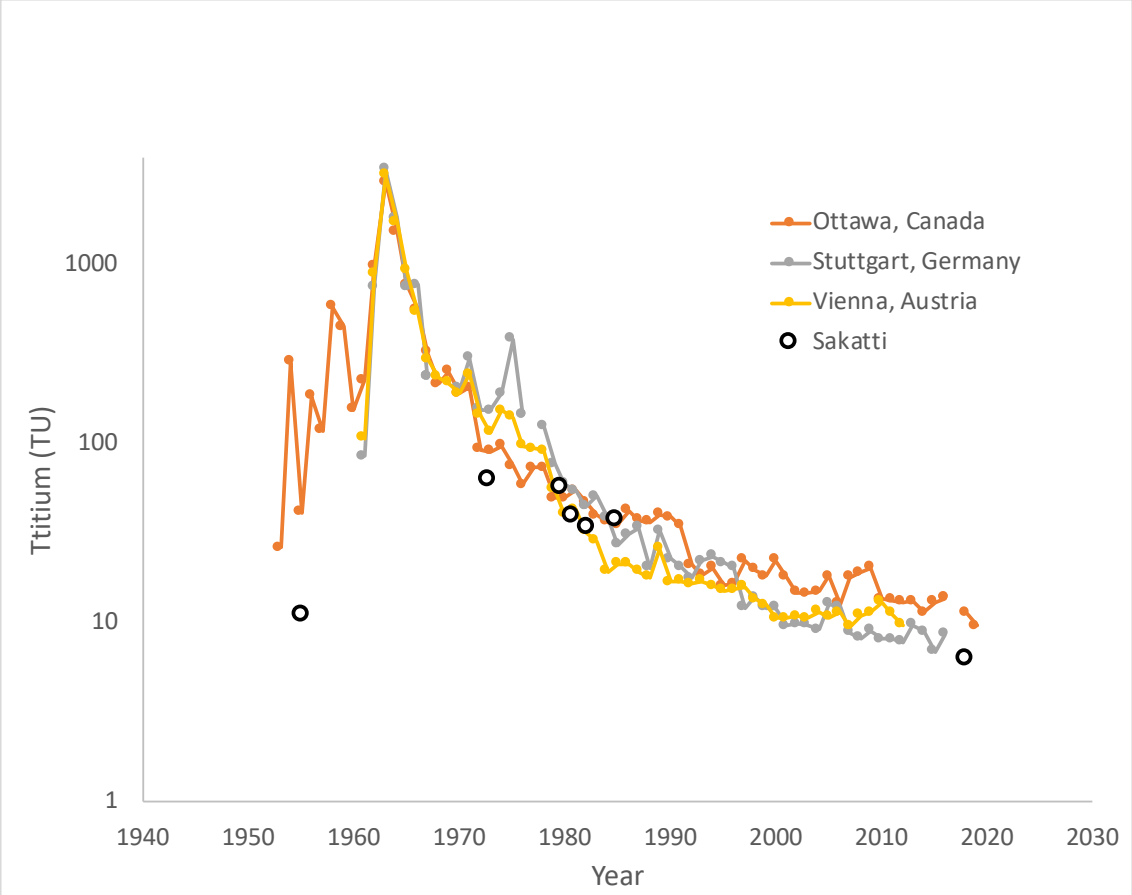

Figure 15. Calculated initial ^{3}H contents in the groundwater samples at Sakatti compared to the contents of ^{3}H in northern hemisphere precipitation in three precipitation stations (International Atomic Energy Agency/World Meteorological Organization, 2019).

Tritium concentrations in precipitation have been declining since the maximum in the 1960's. Hendriksson *et al.* (2014) found concentrations as low as 9.2 TU in precipitation and 7.9 TU in shallow groundwater at Olkiluoto. Data of the GNIP database (International Atomic Energy Agency/World Meteorological Organization, 2019) indicates that the contents of ^{3}H in in precipitation have been ~8-17 TU in Rovaniemi in 2010, ~8-18 in Kuopio in 2010, ~8-21 TU in Espoo in 2010, and 5-15 TU in Poland in 2016.

5.4 CFC-12 and SF_6

The apparent recharge dates based on CFC and SF_6 data is compared in Fig. 16. In case of equal dating results, the samples would lie on the curve drawn for the years 1965–2010. Mixed waters should plot along a line between the two end members lying on the curve. A mixing line between waters recharged in 1965 and 2010 is shown as an example. With two exceptions (D-3-17MOS8193 and D-9-17MOS8193), all samples (M-1-12MOS8102, M-4-12MOS8102, B-5B-GA405, G-6-GA305 and B-11-17HYD013) are located outside the expected area.

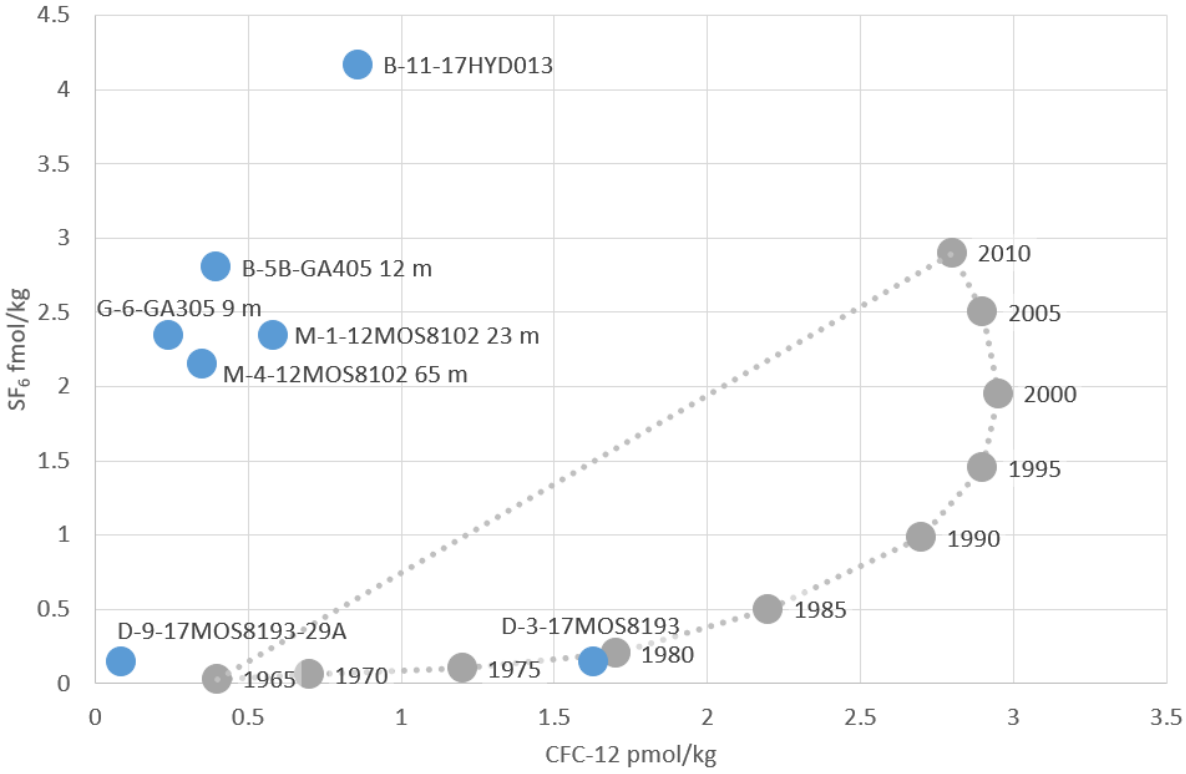

Figure 16. Concentrations of SF_6 and CFC-12 compared to points of equal ages calculated from the two tracers. A mixing line connecting waters recharged in 1965 and 2010 is shown for comparison (based on Plummer and Busenberg 2006, Darling *et al.* 2010).

Excluding these two samples, the SF_6 concentrations exceed 2 fmol kg^{-1}, which suggest apparent recharge dates of later than 2000. These ages are much too young compared

to any other indications from other tracers, including the T/He dated samples B-5B-GA405 and G-6-GA305. The sample B-11-17HYD13 even exceeds the level of the highest possible content of SF_6 in modern precipitation, ~4 fmol l^{-1} (U.S. Geological Survey 2017). The high SF_6 concentrations can be addressed to excess air (Bauer *et al.* 2001), or even more probably, geogenic production of SF_6 in the bedrock. Various rocks, such as fluorite, granite and dolomite are known to be natural sources of SF_6 (Busenberg and Plummer 2000). This makes SF_6 not a suitable tracer for recharge age dating in this kind of an environment, and therefore the SF_6 data is not used for constraining the recharge dates in this study.

CFC samples are extremely vulnerable to contamination. In many studies across different geological settings, samples have been found either contaminated or otherwise influenced by the multiple factors listed in Chapter 3.2.2 that affect the final CFC concentration of groundwater (e.g. Thompson and Hayes 1977, Busenberg and Plummer 1992, Jackson *et al.* 1992, Bauer *et al.* 2001 and many others). In addition, CFCs also degrade microbially over time in anoxic waters, which at the Sakatti area might be present in the mire environment and in the deeper bedrock. In order to evaluate the CFC data, it is critical to compare the analytical results to other age indications.

The CFC concentrations of this study suggest apparent recharge dates of 1960-1980 (Fig. 16). Samples D-3, D-9 and D-11 from 17-MOS8193 represent deep borehole water from a depth of about 900 m. The tritium content in samples D-3 and D-9 was very small or below the detection limit, and the ^{14}C contents indicate an apparent age of >30 000 years. Therefore, the variable CFC-12 concentrations in these samples are attributed to a variable degree of contamination during drilling, sampling, shipping or analysis.

In this study, only two of the shallow wells could be dated using both CFC-12 and tritium methods. Samples B-5B-GA405 and G-6-GA305 had T/He recharge dates of 1975 and 1985, respectively. The apparent dates of recharge suggested by CFC-12 are 1965 and 1962, respectively. In spite of the difference in the results, both methods provide evidence for groundwater recharge during the last 60 years. The small deviation between the two methods could be related to a partial degradation of CFC-12 in an anoxic environment.

Samples M-1-12MOS8102 and M-4-12MOS8102 were collected from the same borehole from depths of 23 m and 63 m, respectively. Their contents of ^{3}H are high suggesting a large component of water recharged at 1960 or later (Table 6). This is confirmed by the contents of CFC-12, which suggest recharge dates of about 1960 to 1970 (Fig. 16). The ^{14}C age for M-4-12MOS8102 is 3 600 cal a BP, and the contents of ^{4}He are high in both samples, giving indications for an ancient origin. These contradictory age indications from the same samples could result from mixing of two different water types with different recharge ages in Borehole 12MOS8102. The sample water from 23 and 65 m being from the fractured upper part of the bedrock, rather than from a specific fracture system, this mixing would be likely.

Favorin (2007) compared dating results of CFC-11, CFC-12 and CFC-113 methods to those of tritium dating method in Virttaankangas ridge formation in southern Finland. She had relatively young samples were tritium dated to be 2.5– 39 years old. Overall, the CFC-12 method was in line with tritium, although it often gave slightly higher ages, but in case of the youngest samples, CFC-12 dating was not possible due to high error margins of the analysis. Szabo *et al.* (1996) similarly compared CFC dating methods to tritium method in <60 m thick sand deposits of southern New Jersey coastal plain. Many of the samples were contaminated, but otherwise their CFC-12 results gave generally younger ages than tritium, average being by 5.3 years, in samples tritium dated to be 2.5–40 years old.

5.5 Groups

The samples were divided into three groups based on their ion composition characteristics in Chapter 5.1 (Fig. 13).

5.5.1 Group 1

The brackish deep groundwaters of Group 1 were pumped from a depth of 950 m. Two of the samples (D-3-17MOS8193 and D-9-17MOS8193) were analysed for ^{14}C, T/He and CFC-12. The contents of tritium were very low and those of ^{4}He very high, making the measurement of tritiogenic ^{3}He impossible, but indicating strongly that the water has

been recharged much before 1950. The concentrations of CFC-12 were low for D-9-17MOS8193 but relatively high for D-3-17MOS8193, the latter possibly related to contamination. The contents of ^{14}C are also low, suggesting an apparent calibrated age of ca. 32 000 years. Due to possible minor contamination by modern carbon during sampling this is a minimum age estimate for this water type.

The isotopic composition of hydrogen and oxygen in the samples of Group 1 are close to those in the present-day precipitation and local groundwaters (Fig. 14). Without doubt, the samples of Group 1 represent the oldest water type in this study. No definitive evidence for mixing with modern or recent groundwaters exists.

5.5.2 Group 2

Based on the δ^2H and $\delta^{18}O$ values, the samples of Group 2 represent evaporated surface waters, except for B-11-17HYD013, which is similar to present-day precipitation (Fig. 14). As with the Group 1 samples, the samples M-1, -2, -4 (12MOS8102) and B-11-17HYD013 have relatively high contents of ^4He (Table 6), possibly related to the presence of an old groundwater component. However, the tritium contents are significantly above zero, from 1.4 to 6.5 TU, providing evidence for a young groundwater component recharged after 1960 (Table 6). The T/He ages could not be calculated for M-1, -2, -4 (12MOS8102) and B-11-17HYD013, due to high contents of ^4He. For samples B-5-GA405, B-13-17HYD004 and G-6-GA305 the T/He ages suggest recharge dates from 1973 to 1981.

The CFC-12 recharge years vary from 1963–1975, which do not completely agree but are roughly in line with the T/He recharge estimates. In contrast, the radiocarbon content for the water sample M-4-12MOS8102 suggests an age of more 3 000 years, providing evidence for an old groundwater component.

Most of the groundwater samples in Group 2, with one exception represent bedrock borehole waters from depths varying from 12 to 96 m. The evaporated δ^2H - $\delta^{18}O$ character of this water type cannot result from processes in the bedrock, but instead it has to be the result of a recharge of evaporated surface water. The sampling sites for all samples in Group 2 are located close to the River Kitinen. The likely source for

evaporated surface water are the open water pools of the local mires (Gat and Tzur 1967, Gonfiantini 1986). According to Åberg S. *et al.* (2017) and Åberg *et al.* (2019), the surface and groundwater flow direction in the area is from the mire to the River Kitinen. T/He and CFC data indicate that the flow has been active during the last 40–60 years, and it has possibly reached a depth of nearly 100 m, as evidenced by the δ^2H and $\delta^{18}O$ data from sample M-2-12MOS8102.

Group 2 samples are dispersed on a Piper diagram (Fig. 17). The borehole 12MOS8102 samples M-1, -2 and -4 are displaced from the other samples towards the location of the Group 1 samples. Although chemically identified with the Group 2 samples, the samples M-1, -2 and -4 (12MOS8102) also have characteristics similar to the deep brackish waters of Group 1. This result could be understood to result from mixing of shallow evaporated water with deep brackish waters, and it is in agreement with the dating results giving indications for both old and recent waters in the same samples.

The borehole sample B-11-17HYD013 is very different from all other samples, containing a much higher content of Cl and SO_4. The anomaly is local, as the feature is missing from a nearby borehole sample B-10-17HYD17. To discover the cause of the anomalous composition would require further studies.

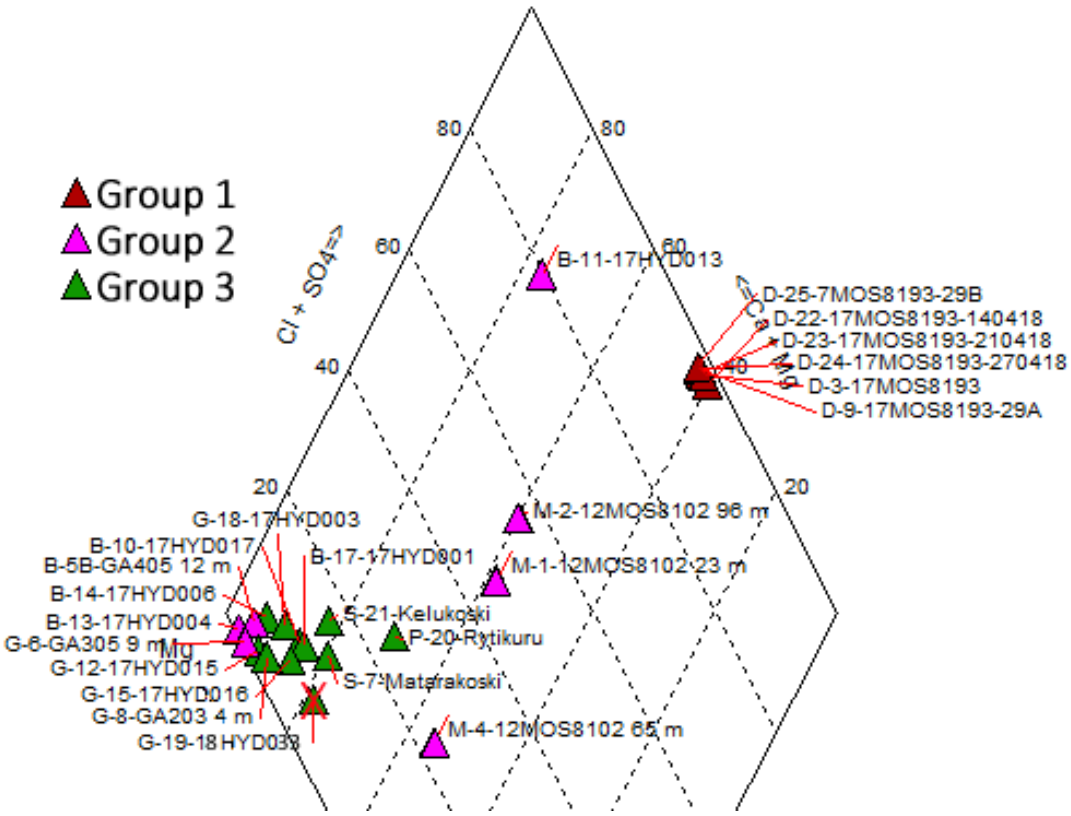

Figure 17. A piper diagram with the samples divided into the groups defined by the ionic composition. AquaChem 2014.2 (15.204.1025).

5.5.3 Group 3

Group 3 contains waters from variable sources, including river water, shallow groundwater in the sedimentary cover and groundwater in the bedrock. A majority of the δ^2H and $\delta^{18}O$ values for the water samples in Group 3 are located close to the composition of the average precipitation, but samples B-14-17HYD006, S-7-Matarakoski and G-12-17HYD015 are distributed along the evaporation trend (Fig. 14). Water samples B-10-17HYD017 and B-14-17HYD006 have been dated using the T/He method. The T/He analysis for sample B-10-17HYD017 suggests mean recharge in 1955, and for the sample B-14-17HYD006 the estimated recharge time is 2018. The dates are generally in line with the tritium contents of 0.32 and 6.39 TU, respectively. The very low tritium concentration of B-10-17HYD017 verifies no significant interaction with recent surface waters. Given the well 17HYD006 is about 100 m deep with screen below bedrock surface at depth of 30–100 m, the sample B-14-17HYD006 being tritium dated to be very

recently is strange. B-14-17HYD006 is clearly more evaporated than the adjacent G-15-17HYD016 (Fig. 14), so the cause is likely a relatively rapid groundwater flow from the vicinity of the mire, but a definitive answer would require additional sampling. According to Åberg *et al.* (2019b), construction of hydro-electric power plants and regulation of the river since the 1970s ended the spring floods of the River Kitinen. However, these floods could have affected the groundwater in the vicinity of the River Kitinen and their past influence need to be further studied, as well.

The water samples of Group 3 include recent surface water samples as well as groundwater samples, which according the two T-He ages may have been recharged during the last 65 years. Two groundwater samples show an evaporated surface water signal (B-14-17HYD006, G-8-GA203), suggesting similarity to the samples of Group 2. Samples from wells and boreholes (B-10-17HYD017, B-17-17HYD001, G-18-17HYD003, G-19-18HYD033, P-20-Rytikuru) have $\delta^{2}H$ and $\delta^{18}O$ values relatively close to those of the local average precipitation (Fig. 14).

The water samples in Group 3 likely represent relatively young groundwaters with a short residence time. In the case of the sample B-10-17HYD017, the recharge age could be as high as 65 years. Evaporated surface water influence can be observed in two groundwater samples (G-8-GA203, G-12-17HYD015) located near the river channel. However, similarly to Group 2, based on the hydrological gradient from the mire towards the River Kitinen, the source of the signal is most likely caused by water permeated from surface water pools in surrounding mire areas.

5.6 Trace elements

In a cluster analysis (Fig. 18), trace element contents of the samples do not correlate with sample source types quite as well as ion composition does (Fig. 13), as trace elements are more dependent on the local geochemical variability of the bedrock. The deep, brackish waters from borehole 17MOS8139 do still form their own distinctive group separate from all the other samples. Shallow bedrock borehole samples B-5B-GA405, B-10-17HYD017 and B-13-17HYD004 are significantly separated from the rest of the samples, and shallow groundwater wells G-6-GA305, G-15-17HYD016, G-19-

18HYD33, and G-18-17HYD003 form their own group. Two samples from 12MOS8102, M-1 and -2 (23 and 96 m), are paired, but the third, M-4 (65 m), is well separated. B-11-17HYD013, which by ion chemistry is clearly separated from all the other shallow sediment and bedrock wells, is paired with M-4, the 12MOS8102 sample furthest from B-11-17HYD013 by ion composition. River water samples S-7 and S-21, together with other Ion Group 3 samples B-14-17HYD006, G-8-GA203 and G-12-17HYD-15 are also grouped together. The rest of the Ion Group 3 samples and all Ion Group 2 samples are spread around without clear correlation.

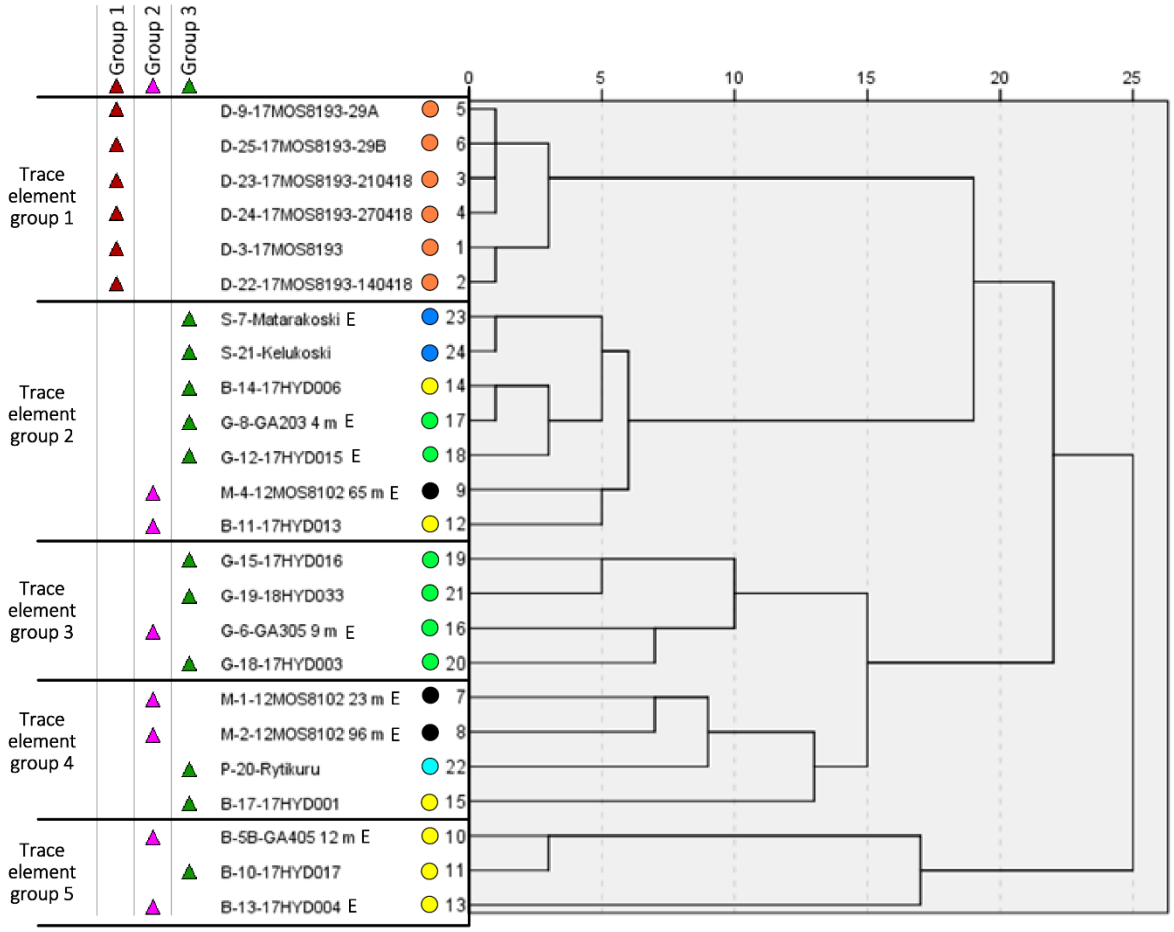

Figure 18. Dendrogram based on trace element contents of the samples using hierarchical clustering (Ward linkage, Euclidean distance, standardized range 0 to 1). Due to low content of Se, Pb and U in most of the samples, they were removed from the analysis. Waters interpreted to have been affected by evaporation (based on δ^2H and $\delta^{18}O$) are marked with a letter E. Samples were divided into three groups by main ion composition in Fig. 13. (marked with triangles). Symbol colors of samples as in Fig. 4. SPSS 25.0.0.1.

Comparing the properties of different groups defined by trace element composition (Fig. 18) it is possible to see what elements define each group (Fig. 19). The most defining elements are Si, Cu, Mo, Cd. The compositions within Trace element Groups 4 and 5 are less consistent, while in case of Trace element Groups 1 and 2 they are very consistent.

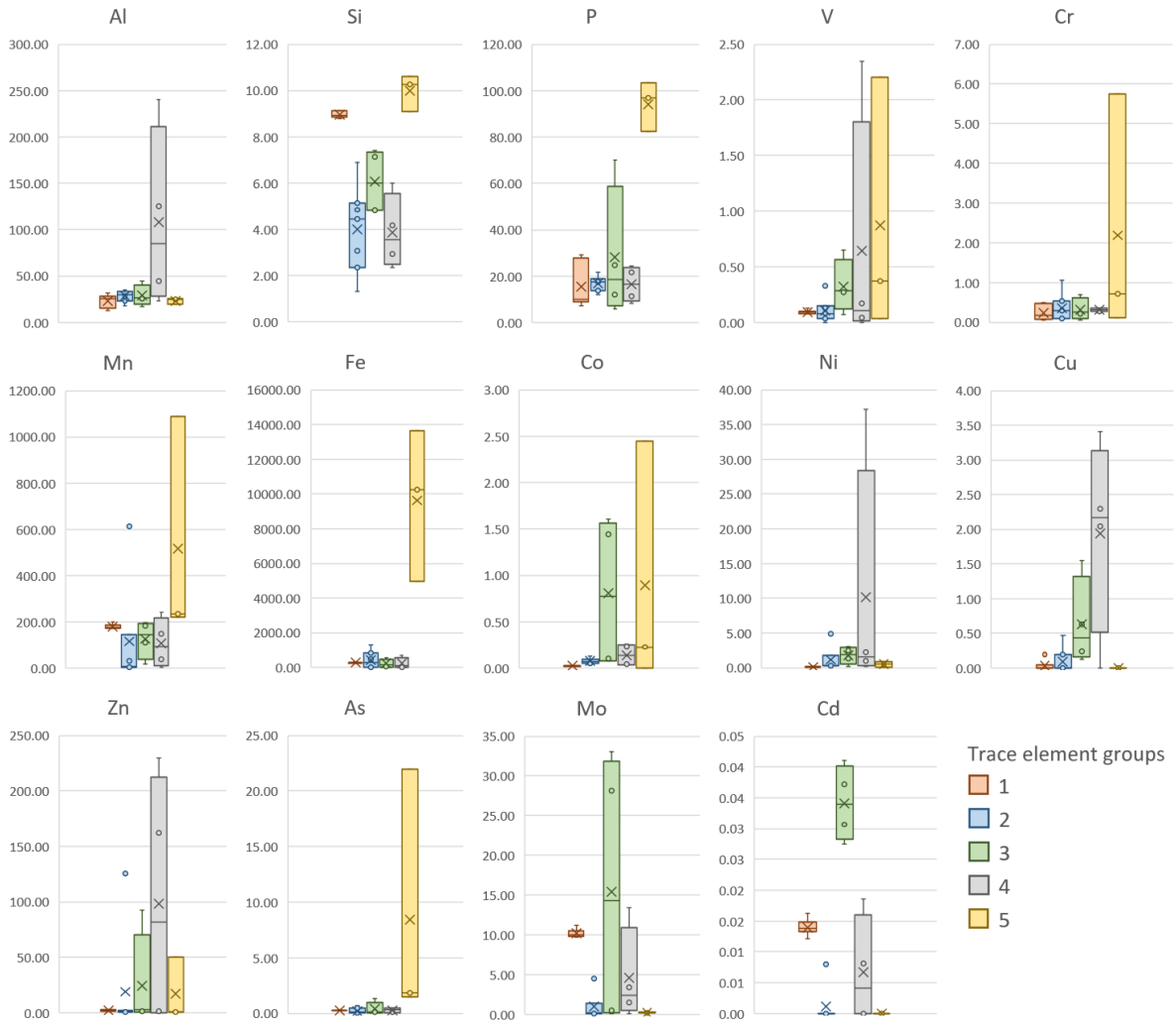

Figure 19. Box plots based on the trace element compositions of the samples. The samples were divided into groups based on the dendrogram in Fig. 18.

Sample B-11-17HYD013 contained the most U of all groundwater samples, 1.03 ppb, which is comparable to the 0.74–0.99 ppb drawn from 17MOS8193. This is in line with other analyses indicating the sample to be a mixture of old and young groundwater due to containing 1.49 TU of tritium and high amount of ^{4}He. It is also the only shallow groundwater sample not of bicarbonate type.

Samples B-5-GA405, B-5B-GA405, B-10-17HYD017 and B-13-17HYD004 had high contents of Si, P, and Fe, as well as As content of >1.45 ppb. B-13-17HYD004 also had exceptionally high V, Cr, Mn and Co contents, and As content of 21.93 ppb. Amount of

M-2 (96 m) was the only sample to contain any measurable Pb, including the other two samples from 12MOS8102, M-1 (23 m) and M-4 (65 m). M-2 also has more Al, P, V, Zn and U than the other two samples, as well as considerably less Fe. Aside from being caused by different sampling depths, the differences could be due to poor sample retriever used in case of only the sample M-2, as there was no possibility to change the water in the well prior to sampling. The retriever also could not fill an entire trace element sample bottle in one go, so additional retrievals were required resulting in mixing of water in the borehole and increased contamination risk while filling the bottle.

M-1 contained more Mn, Co, Ni, Mo and Cd, and less Al, Si, P, As and U, than M-2 and M-4. The differences in Ni and Mo contents were most significant, as M-1 contained 37.17 ppb of Ni, whereas M-2 and M-4 only contained 2.21 and 0.29 ppb, and M-1 contained 13.40 ppb of Mo, while M-2 and M-4 contained only 3.36 and 4.53 ppb. Low contents of As and U would suggest slightly younger groundwater, as would be expected from a sample from upper parts of the borehole.

5.6.1 17MOS8193

The trace element composition of 17MOS8193 remained mostly stable over the 3-week test pumping, although small but clear decrease was observed in the contents of P, V, Mn, Fe, Co, Ni, Zn, As, Mo, Cd and U (Fig. 20). Al, which has an ambiguous rising trend, is likely in suspension and not dissolved, and could reflect the presence of clay minerals (Cabrera and Talibudeen 1978). Cr varied without clear trend. D-23-17MOS8193 was the only sample to contain any measurable Cu. No Se or Pb was found in 17MOS8193, and the remaining element, Si, remained stable. The slight but notable decrease in contents of most elements could indicate slightly more diluted groundwater, or a portion of it, introduced to the system. The ^{14}C method suggested D-9-17MOS8193 (29.4.18) to be ~2 000 years younger than D-3-17MOS8193 (14.4.18). As discussed in Chapter 4.4, these ^{14}C ages could be caused by contamination of the samples, but the decline in trace element content is clear.

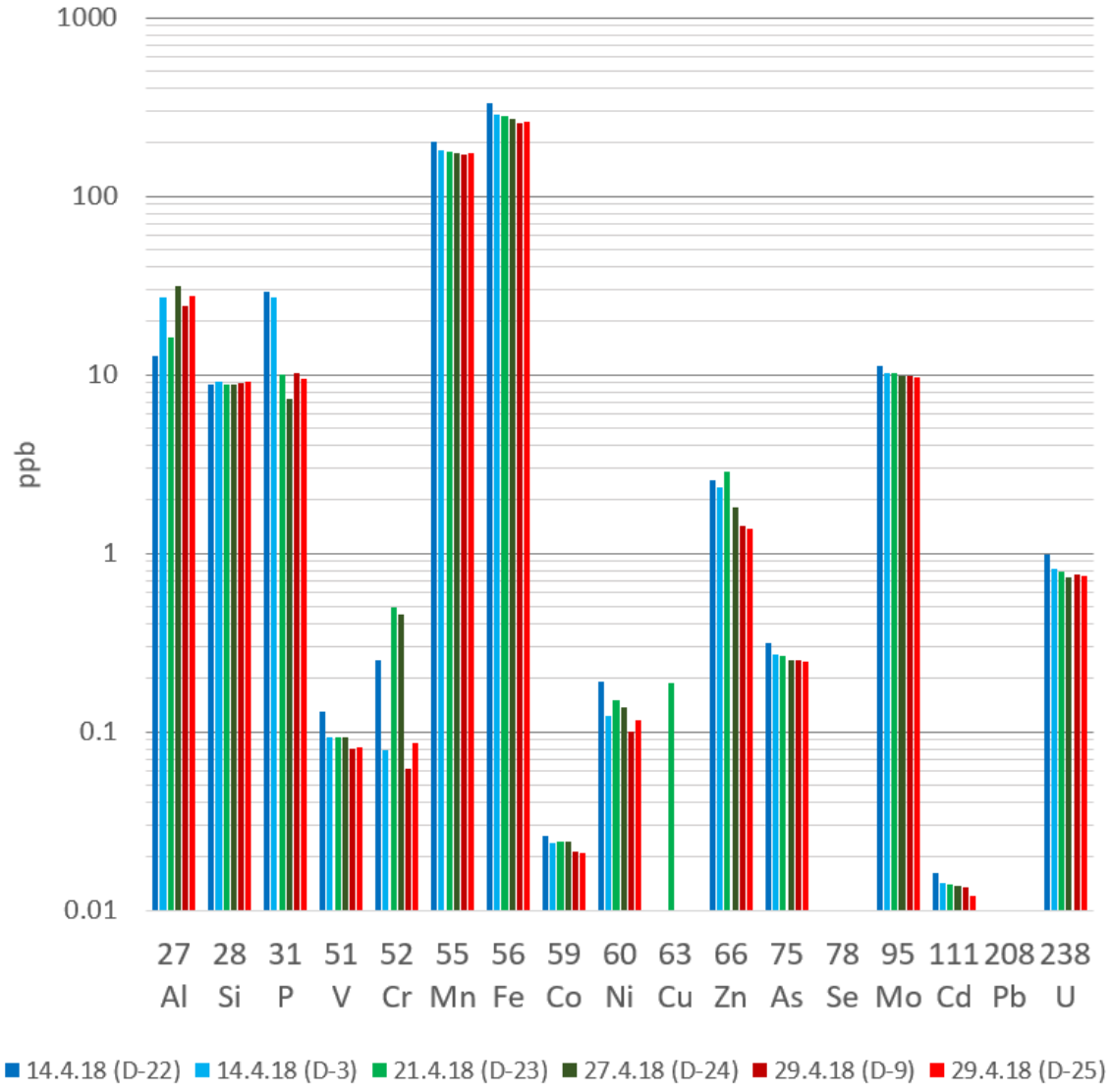

Figure 20. Trace element composition development in 17MOS8193 during the 3-week test pumping.

6. CONCLUSIONS

Various methods exist for studying the recharge age of groundwaters. Unfortunately, interpretation of the data is often not straightforward. Although groundwaters often are mixtures of waters with different infiltration ages, only a single recharge date estimate is obtained. In addition, the tracers may have additional sources or sinks in the groundwater system. Tracer methods also are sensitive to contamination during drilling, sampling and transport. The reliability of the interpretations is increased, if different

methods give similar results and if the dates can be connected to the chemical or isotopic characteristics of the water type.

The deepest groundwater samples from a depth of about 900 m represent the oldest water type in this study. Radiocarbon analyses suggest a minimum age ca. 32 000 years, but the real age could be higher by orders of magnitude. This water type has $\delta^{2}H$ and $\delta^{18}O$ values similar to those in the present-day mean annual precipitation, indicating that the environmental conditions during their infiltration probably were similar to those of today. No clear signs of admixture with modern recharge can be observed.

The $\delta^{2}H$ and $\delta^{18}O$ values of many shallow groundwaters in the sedimentary cover and in the bedrock give strong indications of evaporated surface water infiltration into the sedimentary cover and upper fractured bedrock. The T/He and CFC-12 analyses provide evidence for active recharge during the past 40-60 years. Based on earlier work on groundwater flow (Åberg S. *et al.* 2017), the source of the groundwater with evaporated signal is interpreted flow from the mire towards the River Kitinen. This surface-derived water circulation has reached a depth of nearly 100 m. All sites with a demonstrated presence of recent evaporated surface water infiltration are located within a distance of <200 m from the river channel. Groundwater samples without evaporated signal are mainly from Kuusivaara further south (except G-15-17HYD016 further north, and B-10-17HYD017 west of the river). Former studies in the area show evaporated groundwater is also often found in the mire, further from the river (Åberg *et al.* 2019a). The surface and groundwater flow in the western part of the Viiankiaapa mire is from the mire to the river with a clear gradient (Åberg S. *et al.* 2017), so the infiltration from the river to reach wells east of the channel would require exceptional flow patterns. However, the possible effects of previous pre-regulation floodings of River Kitinen should be examined in future, as well.

Shallow groundwater wells generally have $\delta^{2}H$ and $\delta^{18}O$ values similar to those in the mean annual precipitation (except B-5B-GA405, G-6-GA305, G-8-GA203, G-12-17HYD015 and B-13-17HYD004). This water type is relatively young, and the recharge has occurred within the last 70 years.

As is apparent from the complications and results of the study, it is essential to use as wide range of methods as possible. Especially in cases where both recently and thousands of years ago recharged waters exist, no single method could even cover the entire potential time span. Every dating method has its advantages and shortcomings, and the results of one method cannot be completely trusted without cross confirming via other methods. The T/He method provided accurate results for the younger samples, and while it could not determine exact ages of some samples, it was enough to figure out estimates in light of other results. ^{14}C was known, and proved to be, a reliable way to date older groundwaters. CFC method did not yield accurate groundwater ages, but gave reliable approximates, also cross-verifying the results of both tritium and ^{14}C methods. Where tritium analysis was not able to determine date, CFC method still gave rough estimates. Geogenic SF6 generation is clear in the area, at least the deepest boreholes, and the method is not viable for any interpretation in the area.

While dating methods give an image of the situation, knowing the full chemistry of the water is always crucial in determining the factors that led to it. Tracing back the history of individual samples was made possible. Isotope ratios tell the precipitation, recharge and evaporation history of the water, and thus hint at the sources, residence areas and flow paths. Ion composition divided the samples into distinct groups and shows how certain samples are connected or not to each other, confirming the mixed nature of certain waters. Trace elements deepened this knowledge about the samples' relation to each other, and showed an introduction of slightly diluted water in 17MOS8193.

Continuous monitoring of $\delta^{2}H$ and $\delta^{18}O$ in select wells could give useful information on the recharge patterns in the area. Measuring the delay of a well to react to the annual isotope cycle, such as the significant change during the snow melt period, could give more indication of the infiltration source of the groundwater and the connections of the wells and aquifers as well.

7. AKNOWLEDGEMENTS

From the University of Helsinki, I would like to thank Kirsti Korkka-Niemi and Juha Karhu for supervising this thesis, and for providing all the valuable help and guidance. I am grateful to AA Sakatti Mining Oy for providing and financing this study, and Anne Rautio for the assistance and contribution on their part. I would also like to thank the laboratory personnel of the University of Helsinki for the analysis of the samples. Lastly, I wish to thank my family and friends for the support and pressure during the whole process.

REFERENCES

Åberg, A., Åberg, S., Salonen, V.-P., Korkka-Niemi, K., Rautio, A. and Koivisto, E. 2017. GIS-based 3D sedimentary model for visualizing complex deposition in Kersilö, Finnish Lapland. Boreal Environment Research 22, 277–298.

Åberg, S., Åberg, K., Korkka-Niemi, K. and Salonen, V.-P. 2017. Hydrostratigraphy and 3D modelling of a bank storage affected aquifer in mineral exploration area in Sodankylä, northern Finland. In: Wolkersdorfer, C., Sartz, L., Sillanpää, M. and Häkkinen, A. Mine water and circular economy. International Mine Water Association Congress, Lappeenranta, 237–243.

Åberg, S., Korkka-Niemi, K., Rautio, A., Salonen, V.-P. and Åberg, A. 2019a. Groundwater recharge/discharge patterns and groundwater–surface water interactions in a sedimentary aquifer along the River Kitinen in Sodankylä, northern Finland. Boreal Environment Research 24, 155–187.

Åberg S., Korkka-Niemi, K., Rautio, A., Salonen, V.-P. and Åberg, A. 2019b. The regulation of the River Kitinen to flood affected Mire Viiankiaapa, Sodankylä. In: Kalliomäki, H. (editor). Proceedings of the Geological Society of Finland volume 1, abstracts of the 5th Finnish national colloquium of geosciences.

Ahonen, L., Kietäväinen, R., Kortelainen, N., Kukkonen, I. T., Pullinen, A., Toppi, T., Bomberg, M., Itävaara, M., Nousiainen, A., Nyyssönen, M. ja Öster, M. 2011. Hydrogeological characteristics of the Outokumpu Deep Drill Hole. Geological Survey of Finland, Special Paper 51, 151–168.

Åkesson, M., Suckow, A., Visser, A., Sültenfuβ, J., Laier, T., Purtschert, R. and Sparrenbom, C. 2015. Journal of Hydrology 528, 217–229.

Alanne, M., Honka, A. and Karjalainen, N. 2014. Lokan ja Porttipahdan tekojärvien säännöstelyn kehittäminen – Yhteenveto ja toimenpidesuositukset. Lapin elinkeino-, liikenne- ja ympäristökeskus, Raportteja 38.

Bauer, S., Fulda, C. and Schäfer, W. 2001. A multi-tracer study in a shallow aquifer using age dating tracers 3H, 85Kr, CFC-113 and SF6 – indication for retarded transport of CFC-113. Journal of hydrogeology 248, 14–34.

Bethke, C. and Johnson, T. 2008. Groundwater age and groundwater dating. Annual Review of Earth and Planetary Sciences 36, 121–152.

Blomqvist, R., Lahermo, P., Lahtinen, R. and Halonen, S. Geochemical profiles of deep groundwater in Precambrian bedrock in Finland. Geological Survey of Finland, Report YST-58, 29 p.

Blomqvist, R. 1999. Hydrogeochemistry of deep groundwaters in the central part of the Fennoscandian Shield. Geological Survey of Finland, Report YST-101, 41 p.

Brownscombe, W., Ihlenfeld, C., Coppard, J., Hartshorne, C., Klatt, S., Siikaluoma, J. and Herrington, R. 2015. The Sakatti Cu-Ni-PGE sulfide deposit in Northern Finland. In: Maier, W., Lahtinen, R. and O'Brien, H. (editors) Mineral deposits of Finland. Elsevier, Amsterdam, 211–252.

Busenberg, E. and Plummer, L. 1992. Use of chlorofluorocarbons (CCl_3F and CCl_2F_2) as hydrologic tracers and age-dating tools: the alluvium and terrace system of central Oklahoma. Water resources research 28, 2257–2283.

Busenberg, E. and Plummer, L. 2000. Dating young groundwater with sulfur hexafluoride: natural and anthropogenic sources of sulfur hexafluoride. Water Resources Research 36, 3011–3030.

Cabrera, F. and Talibudeen, O. 1978. The release of aluminium from aluminosilicate minerals. II. Acid-base potentiometric titrations. Clays and clay minerals 27, 113–118.

Cook, P., Plummer, L., Solomon, D., Busemberg, E. and Han, L. 2006. Effects and processes that can modify apparent CFC age. In: International Atomic Energy Agency, Use of chlorofluorocarbons in hydrogeology – a guidebook. International Atomic Energy Agency, Vienna, 276 p.

Darling, W., Gooddy, D., Morris, B. and MacDonald, A. 2010. Using CFCs and SF6 for groundwater dating: a SWOT analysis. Water-rock interaction 13, 15–22.

Friedman, I. 1953. Deuterium content of natural waters and other substances. Geochimica et Cosmochimica Acta 4, 89–103.

Gat, J. and Tzur, Y. 1967. Modification of the isotopic composition of rainwater by processes which occur before groundwater recharge. In: Isotopes in hydrology. International Atomic Energy Agency, Vienna, 49–60.

Geological Survey of Finland 2010. Superficial deposits of Finland 1:200 000. Accessible at: https://hakku.gtk.fi/.

Geological Survey of Finland 2017. Bedrock of Finland 1:200 000. Accessible at: https://hakku.gtk.fi/.

Gonfiantini, R. 1986. Chapter 3 - Environmental isotopes in lake studies. In: Handbook of environmental isotope geochemistry, the terrestrial environment, B. Elsevier, Amsterdam, 113–168.

Graig, H. 1961. Isotopic variations in meteoric waters. Science 133 (3465), 1702–1703.

Healy, R. 2010. Estimating groundwater recharge. Cambridge University Press, Cambridge, 256 p.

Heilweil, V., Solomon, D., Gingerich, S. and Verstraeten, I. 2009. Oxygen, hydrogen, and helium isotopes for investigating groundwater systems of the Cape Verde Islands, West Africa. Hydrogeology Journal 17, 1157–1174.

Hendriksson, N., Karhu, J. and Niinikoski, P. 2014. ^{18}O, ^{2}H and ^{3}H isotopic composition of precipitation and shallow groundwater in Olkiluoto. Working report 2014-69. Posiva Oy, Eurajoki.

Hirvas, H. 1991. Pleistocene stratigraphy of Finnish Lapland. Geological Survey of Finland, Espoo, 123 p.

International Atomic Energy Agency 2013. Isotope methods for dating old groundwater. International Atomic Energy Agency, Vienna, 357 p.

International Atomic Energy Agency/World Meteorological Organization 2019. Global Network of Isotopes and Precipitation. The GNIP Database. Accessible at: https://nucleus.iaea.org/wiser.

Jackson, R., Lesage, S. and Priddle, M. 1992. Estimating the fate and mobility of CFC-113 in groundwater: results from the Gloucester landfill project. In: Lesage, S. and Jackson, R. (editors) Groundwater contamination and analysis at hazardous waste sites. Marcel Dekker, New York, 511–526.

Kalin, R. 2000. Radiocarbon dating of groundwater systems. In: Cook, P. and Herczeg A. (editors) Environmental tracers in subsurface hydrology. Kluwer Academic Press, Boston, 111–144.

Kortelainen, N. 2007. Isotopic fingerprints in surficial waters: stable isotope methods applied in hydrogeological studies. Geological Survey of Finland, Espoo.

Kortelainen, N. and Karhu, J. 2004. Regional and seasonal trends in the oxygen and hydrogen isotope ratios of Finnish groundwaters: a key for mean annual precipitation. Journal of Hydrology 285, 143-157.

Lahtinen, T. 2017. Hydrogeochemical characterization of the Sakatti mine prospecting area, Sodankylä, Finnish Lapland. Master Thesis. University of Helsinki, Department of geosciences and geography.

Metsähallitus 2006. Viiankiaavan hoito- ja käyttösuunnitelma. Metsähallituksen luonnonsuojelujulkaisuja C 11.

Niswonger, R., Panday, S. and Ibaraki, M. 2011. MODFLOW-NWT, a Newton formulation for MODFLOW-2005. In: U.S. Geological Survey Techniques and Methods 6-A37, 44 p.

Pearson, F. and Hanshaw, B. 1970. Sources of dissolved carbonate species in groundwater and their effects on carbon-14 dating. In: International Atomic Energy Agency, Isotope hydrology. IAEA, Vienna, 271–286.

Plummer, L., Michel, R., Thurman, E. and Glynn, P. 1993. Environmental tracers for age dating young ground water. In: Alley, W.M. (editor) Regional ground-water quality. Van Nostrand Reinhold, New York, 255–294.

Plummer, L. and Busenberg, E. 2000. Chlorofluorocarbons. In: Cook, P. and Herczeg A. (editors) Environmental tracers in subsurface hydrology. Kluwer Academic Press, Boston, 441–478.

Plummer, L. 2005. Dating of young groundwater. In: Aggarwal, P., Gat, J. and Froehlich, K. (editors), Isotopes in the water cycle: past, present and future of a developing science. Springer, Dordrecht, 193–218.

Plummer, L. and Busenberg, E. 2006. Chlorofluorocarbons in the atmosphere. In: International Atomic Energy Agency, Use of chlorofluorocarbons in hydrogeology – a guidebook. International Atomic Energy Agency, Vienna, 276 p.

Plummer, L., Busenberg, E. and Cook, P. 2006. Principles of chlorofluorocarbon dating. In: International Atomic Energy Agency, Use of chlorofluorocarbons in hydrogeology – a guidebook. International Atomic Energy Agency, Vienna, 276 p.

Reimer, P., Bard, E., Bayliss, A., Beck, J., Blackwell, P., Bronk Ramsey, C., Grootes, P., Guilderson, T., Haflidason, H., Hajdas, I., HattŽ, C., Heaton, T., Hoffmann, D., Hogg, A., Hughen, K., Kaiser, K., Kromer, B., Manning, S., Niu,, Reimer, R., Richards, D., Scott, E., Southon, J., Staff, R., Turney, C.

& van der Plicht, J. 2013. IntCal13 and Marine13 Radiocarbon Age Calibration Curves 0-50,000 Years cal BP. Radiocarbon, 55, 1869–1887.

Schlosser, P., Stute, M., Dörr, H., Sonntag, C. and Münnich, K.O. 1988. Tritium/^{3}He dating of shallow groundwater. Earth and planetary science letters 89, 353–362.

Schlosser, P., Stute, M., Sonntag, C. and Münnich, K.O. 1989. Tritiogenic ^{3}He in shallow groundwater. Earth and planetary science letters 94, 245–256.

Solomon, D. and Cook, P. 2000. ^{3}H and ^{3}He. In: Cook, P. and Herczeg, A. (editors) Environmental tracers in subsurface hydrology. Kluwer Academic, Boston, 397–424.

Thilo, L. and Münnich, K. 1970. Reliability of carbon-14 dating of groundwater: effect of carbonate exchange. In: International Atomic Energy Agency, Isotope Hydrology. International Atomic Energy Agency, Vienna, 917 p.

Thompson, G. and Hayes, J. 1977. Trichlorofluoromethane in groundwater – a possible indicator of groundwater age. Purdue University Water Resources Research Center, Technical report 90.

University of Bremen 2016. Notes for sampling. Available at: https://www.noblegas.uni-bremen.de/eng/downloads/hints_for_sampling_2016.pdf

U.S. Geological Survey 2017. Air Curves CFCs SF6 3H excel spreadsheet. Visited 20.5.20. Available at: https://water.usgs.gov/lab/software/air_curve/

APPENDIX

Appendix 1. Profiles of some of the groundwater wells.

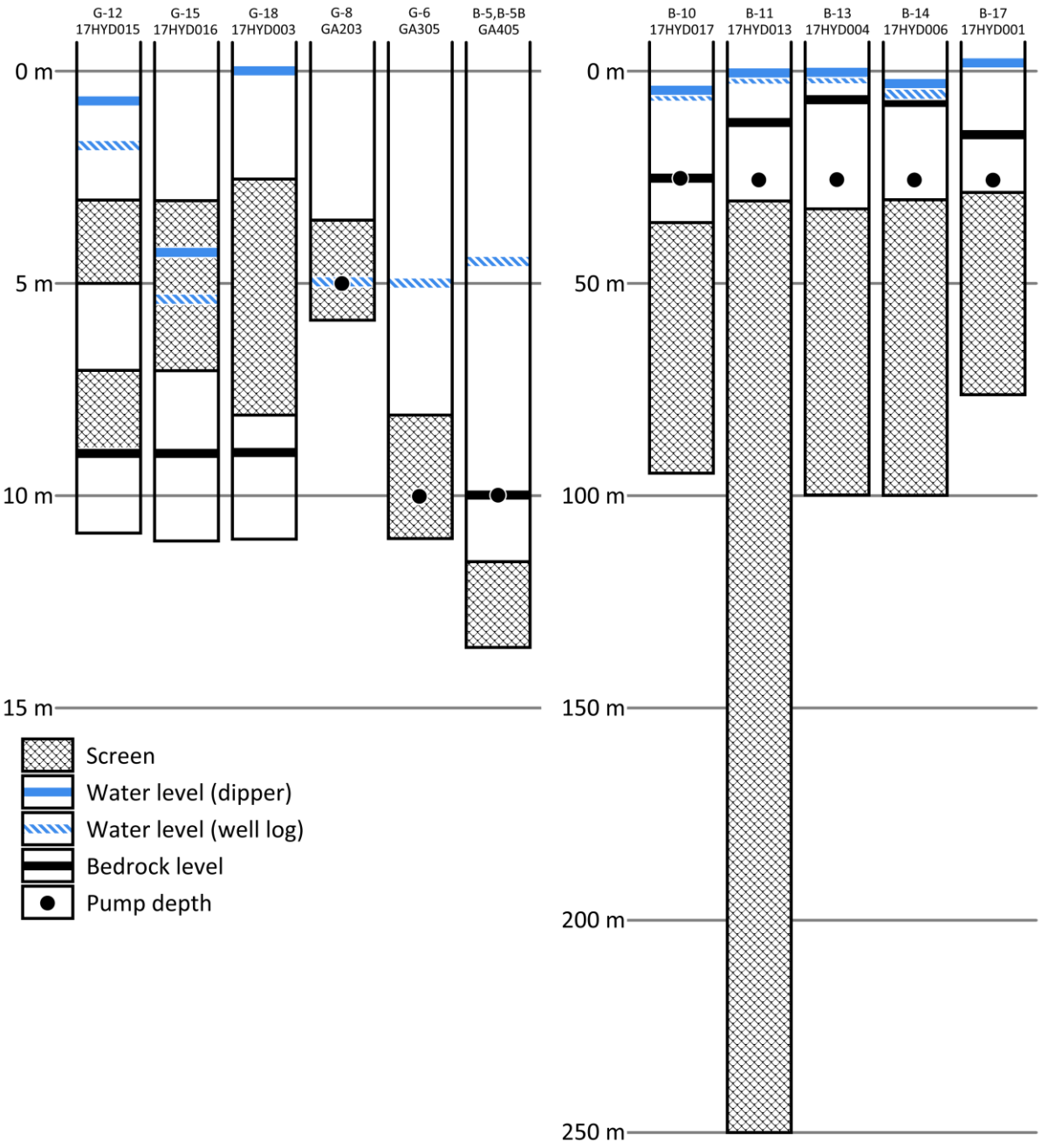

Appendix 2. Measurement and analysis results for R-16-Ruosteoja.

			Field measurement			Lab analysis
δ^2H (‰, VSMOW)	$\delta^{18}O$ (‰, VSMOW)	D-excess (‰)	T (°C)	pH	EC (mS/cm)	EC (mS/cm)
-97.7	-12.62	3.3	9.7	6.53	0.285	0.342

Cations	mg/l				**Anions**	mg/l			
Na	K	Ca	Mg	pH (lab)	F	Cl	NO_3	PO_4	SO_4
33.01	0.33	17.09	7.64	6.52	0.03	49.15	<0.1	0.00	62.85

			Ionic sum meq/l		
Alk. mmol/l	Alk. as $CaCO_3$ mg/l calc.	HCO_3 mg/l calc.	∑Cations	∑Anions	IB%
0.31	15.50	18.91	2.93	3.01	1.37

Trace elements (ppb)								
27 Al	**28 Si**	**31 P**	**51 V**	**52 Cr**	**55 Mn**	**56 Fe**	**59 Co**	**60 Ni**
28.48	**4.46**	**24.60**	**0.00**	**0.33**	**93.30**	**253.13**	**1.17**	**1.11**
63 Cu	**66 Zn**	**75 As**	**78 Se**	**95 Mo**	**111 Cd**	**208 Pb**	**238 U**	
0.68	**5.43**	**0.18**	**0.00**	**0.08**	**0.02**	**0.00**	**0.00**	